(latency III). Reproduction of latency III in the present study makes for an interesting contrast with the previous model using NOD/*scid* mice, which exhibited the latency II pattern [10].

EBV infection in lower doses resulted in a transient increase in EBV DNA load in the peripheral blood, followed by apparently asymptomatic infection that persisted for at least 22 weeks. This type of asymptomatic EBV infection has not been described in nonprimate models of EBV infection and may be regarded as a model of human EBV latency. To compare this condition in NOG mice with EBV latency in humans precisely, we need to further investigate the nature of host cells (i.e., whether they are memory B cells), the pattern of EBV gene expression in them, and the involvement of anti-EBV immune responses in its maintenance.

In hNOG mice, human T cells develop in thymus tissue, in which epithelial cells are of murine origin [16]. It is therefore interesting that they could mount a T cell response restricted by human MHC class I. Although this suggests that positive selection of human T cells occurred in hNOG mice, the mechanism of T cell education remains unclear. Alloantigen-specific and human MHC class I–restricted T cell cytotoxicity has been reported in hNOG mice [15, 16]. An EBV-induced T cell response was evident in mice that received high doses of virus and developed lymphoproliferative disorder, suggesting that the T cell response in hNOG mice was not sufficient to control EBV-induced lymphoproliferation when they were infected at high doses. That only a minor fraction of $CD8^+$ T cells appeared to be EBV specific, as evidenced by ELISPOT assay and flow cytometry, may explain this result, at least partially. A humoral immune response to EBV has not been documented in previous mouse models of EBV infection, and therefore the NOG mouse may provide a valuable tool to analyze the mechanism and the protective roles of antibody response in EBV infection. We have to date clearly identified only IgM antibody to the 18-kDa component of virus capsid antigen in a minor fraction (4/30) of infected mice. We are currently attempting to improve sensitivity and to see whether hNOG mice can mount a more efficient and divergent antibody response to the virus, possibly including the production of IgG antibodies. Because both the T cell–mediated and the humoral immune response are elicited in hNOG mice, they may be useful in the evaluation of candidate EBV vaccines.

Very recently, humanized mice based on other immunodeficient mouse strains were prepared, and EBV was used as a typical pathogen to analyze their immune functions. Traggiai et al. [12] infected humanized $Rag2^{-/-}IL\text{-}2R\gamma^{-/-}$ mice with EBV and documented an in vitro proliferative response by $CD8^+$ T cells to an autologous LCL. Melkus et al. [11], on the other hand, humanized NOD/*scid* mice by transplanting human fetal liver, thymus, and HSCs and succeeded in inducing an EBV-specific T cell immune response as well as an innate immune response to toxic shock syndrome toxin 1. These 2 studies were performed mainly using immunological standpoints and did not provide detailed data from virological investigations. An advantage of the NOG mouse model described here is that it does not require a fine surgical procedure using human fetal tissue; therefore, NOG mice can be easily provided in large quantities.

In immunocompromised humans, failure of immunosurveillance may lead to the development of lymphoproliferative disorder. We expect that the NOG mouse model can be used to analyze the exact relationship between immunodeficiency and the development of lymphoproliferative disorder. Immune responses in the hNOG mouse can be modulated by immunosuppressive drugs (such as cyclosporine A) or HIV, and the development of lymphoproliferative disorder can be analyzed with special reference to the nature and level of immunodeficiency. This kind of study, which has not been possible with conventional *scid* mice, may reveal an exact condition in which lymphoproliferative disorder develops and may thereby aid the development of a specified immunosuppressive procedure that evades this condition and precludes the risk of lymphoproliferative disorder.

In summary, the NOG mouse is able to recapitulate various essential elements of human EBV infection and is therefore, to our knowledge, the most comprehensive small-animal model of EBV infection described to date. It should be a valuable tool for the study of the pathogenesis, prevention, and treatment of EBV infection.

Acknowledgments

We thank Satoshi Itakura, Fuyuko Kawano, Eri Yamada, Miki Mizukami, and Ken Watanabe for technical assistance. We thank Shizuko Minegishi for advice on flow cytometry, Atsushi Komano for advise on the enzyme-linked immunospot assay, Ayako Demachi-Okamura and Kiyotaka Kuzushima for advice on detection of Epstein-Barr virus–specific T cells, and Shosuke Imai for helpful discussions. We thank the Tokyo Cord Blood Bank for supplying cord blood.

References

1. Rickinson AB, Kieff E. Epstein-Barr virus. In: Knipe DM, Howley PM, eds. Fields virology. Philadelphia: Lippincott Williams & Wilkins, **2001**: 2575–628.
2. Kieff E, Rickinson AB. Epstein-Barr virus and its replication. In: Knipe DM, Howley PM, eds. Fields virology. 4th ed. Philadelphia: Lippincot Williams & Wilkins, **2001**:2511–74.
3. Young LS, Finerty S, Brooks L, Scullion F, Rickinson AB, Morgan AJ. Epstein-Barr virus gene expression in malignant lymphomas induced by experimental virus infection of cottontop tamarins. J Virol **1989**; 63: 1967–74.
4. Miller G, Shope T, Coope D, et al. Lymphoma in cotton-top marmosets after inoculation with Epstein-Barr virus: tumor incidence, histologic spectrum antibody responses, demonstration of viral DNA, and characterization of viruses. J Exp Med **1977**; 145:948–67.
5. Cho Y, Ramer J, Rivailler P, et al. An Epstein-Barr-related herpesvirus from marmoset lymphomas. Proc Natl Acad Sci USA **2001**; 98:1224–9.
6. Moghaddam A, Rosenzweig M, Lee-Parritz D, Annis B, Johnson RP, Wang F. An animal model for acute and persistent Epstein-Barr virus infection. Science **1997**; 276:2030–3.
7. Mosier DE, Gulizia RJ, Baird SM, Wilson DB. Transfer of a functional human immune system to mice with severe combined immunodeficiency. Nature **1988**; 335:256–9.

8. Okano M, Taguchi Y, Nakamine H, et al. Characterization of Epstein-Barr virus-induced lymphoproliferation derived from human peripheral blood mononuclear cells transferred to severe combined immunodeficient mice. Am J Pathol **1990**; 137:517–22.
9. Rowe M, Young LS, Crocker J, Stokes H, Henderson S, Rickinson AB. Epstein-Barr virus (EBV)-associated lymphoproliferative disease in the SCID mouse model: implications for the pathogenesis of EBV-positive lymphomas in man. J Exp Med **1991**; 173:147–58.
10. Islas-Ohlmayer M, Padgett-Thomas A, Domiati-Saad R, et al. Experimental infection of NOD/SCID mice reconstituted with human CD34+ cells with Epstein-Barr virus. J Virol **2004**; 78:13891–900.
11. Melkus MW, Estes JD, Padgett-Thomas A, et al. Humanized mice mount specific adaptive and innate immune responses to EBV and TSST-1. Nat Med **2006**; 12:1316–22.
12. Traggiai E, Chicha L, Mazzucchelli L, et al. Development of a human adaptive immune system in cord blood cell-transplanted mice. Science **2004**; 304:104–7.
13. Hiramatsu H, Nishikomori R, Heike T, et al. Complete reconstitution of human lymphocytes from cord blood CD34+ cells using the NOD/SCID/γ_c^{null} mice model. Blood **2003**; 102:873–80.
14. Ito M, Hiramatsu H, Kobayashi K, et al. NOD/SCID/γ_c^{null} mouse: an excellent recipient mouse model for engraftment of human cells. Blood **2002**; 100:3175–82.
15. Yahata T, Ando K, Nakamura Y, et al. Functional human T lymphocyte development from cord blood CD34+ cells in nonobese diabetic/Shi-scid, IL-2 receptor gamma null mice. J Immunol **2002**; 169:204–9.
16. Ishikawa F, Yasukawa M, Lyons B, et al. Development of functional human blood and immune systems in NOD/SCID/IL2 receptor γ chain^{null} mice. Blood **2005**; 106:1565–73.
17. Miyazato P, Yasunaga J, Taniguchi Y, Koyanagi Y, Mitsuya H, Matsuoka M. De novo human T-cell leukemia virus type 1 infection of human lymphocytes in NOD-SCID, common gamma-chain knockout mice. J Virol **2006**; 80:10683–91.
18. Watanabe S, Terashima K, Ohta S, et al. Hematopoietic stem cell-engrafted NOD/SCID/IL2Rgamma null mice develop human lymphoid systems and induce long-lasting HIV-1 infection with specific humoral immune responses. Blood **2007**; 109:212–8.
19. Dewan MZ, Terashima K, Taruishi M, et al. Rapid tumor formation of human T-cell leukemia virus type 1-infected cell lines in novel NOD-SCID/gammac^{null} mice: suppression by an inhibitor against NF-kappaB. J Virol **2003**; 77:5286–94.
20. Watanabe S, Ohta S, Yajima M, et al. Humanized NOD/SCID/IL2Rγ^{null} mice transplanted with hematopoietic stem cells under nonmyeloablative conditions show prolonged life spans and allow detailed analysis of human immunodeficiency virus type 1 pathogenesis. J Virol **2007**; 81: 13259–64.
21. Takada K, Ono Y. Synchronous and sequential activation of latently infected Epstein-Barr virus genomes. J Virol **1989**; 63:445–9.
22. Condit RC. Principles of virology. In: Knipe DM, Howley PM, eds. Fields virology. Philadelphia: Lippincott Williams & Wilkins, **2001**:19–51.
23. Kimura H, Morita M, Yabuta Y, et al. Quantitative analysis of Epstein-Barr virus load by using a real-time PCR assay. J Clin Microbiol **1999**; 37:132–6.
24. Nakamura H, Iwakiri D, Ono Y, Fujiwara S. Epstein-Barr-virus-infected human T-cell line with a unique pattern of viral-gene expression. Int J Cancer **1998**; 76:587–94.
25. Kuzushima K, Hoshino Y, Fujii K, et al. Rapid determination of Epstein-Barr virus-specific CD8$^+$ T-cell frequencies by flow cytometry. Blood **1999**; 94:3094–100.
26. van Grunsven WM, Nabbe A, Middeldorp JM. Identification and molecular characterization of two diagnostically relevant marker proteins of the Epstein-Barr virus capsid antigen complex. J Med Virol **1993**; 40: 161–9.
27. Rezk SA, Weiss LM. Epstein-Barr virus-associated lymphoproliferative disorders. Hum Pathol **2007**; 38:1293–304.

T Cell–Mediated Control of Epstein-Barr Virus Infection in Humanized Mice

Misako Yajima,[1] Ken-Ichi Imadome,[1] Atsuko Nakagawa,[2] Satoru Watanabe,[3] Kazuo Terashima,[4] Hiroyuki Nakamura,[1] Mamoru Ito,[6] Norio Shimizu,[3] Naoki Yamamoto,[5] and Shigeyoshi Fujiwara[1]

[1]Department of Infectious Diseases, National Research Institute for Child Health and Development, and [2]Pathology Laboratory, Department of Clinical Laboratory Medicine, National Center for Child Health and Development, Setagaya-ku, [3]Department of Virology, Division of Medical Science, Medical Research Institute, and [4]Department of Pathology, Faculty of Medicine, Tokyo Medical and Dental University, Bunkyo-ku, and [5]AIDS Research Center, National Institute of Infectious Diseases, Shinjuku-ku, Tokyo, and [6]Central Institute for Experimental Animals, Kawasaki, Kanagawa, Japan

Humanized NOD/Shi-*scid*/interleukin-2Rγ^{null} (NOG) mice with full T cell development had significantly longer life span after Epstein-Barr virus (EBV) infection, compared with those with minimal T cell development. Removing CD3$^+$ or CD8$^+$ T cells from EBV-infected humanized mice by administration of anti-CD3 or anti-CD8 antibodies reduced their life span. CD8$^+$ T cells obtained from EBV-infected mice suppressed the outgrowth of autologous B cells isolated from uninfected mice and inoculated with EBV in vitro. These results indicate that humanized NOG mice are capable of T cell–mediated control of EBV infection and imply their usefulness as a tool to evaluate immunotherapeutic and prophylactic strategies for EBV infection.

Epstein-Barr virus (EBV) is a ubiquitous B-lymphotropic herpesvirus, and >90% of the adult population in the world is latently infected with the virus [1]. Although EBV is an important etiological factor in various malignancies, including endemic Burkitt lymphoma, Hodgkin lymphoma, and nasopharyngeal carcinoma, most EBV infection is asymptomatic and persists for life without any signs or symptoms. EBV has a unique ability to transform human B lymphocytes in vitro and to establish immortalized lymphoblastoid cell lines [2]. EBV-transformed lymphoblastoid cell lines express 9 viral proteins, most of which serve as efficient targets of EBV-specific T cell responses [2]. In immunologically competent hosts, therefore, EBV-transformed cells are readily removed by EBV-specific cytotoxic T lymphocytes [3], and EBV persistence is restricted to memory B cells, in which the expression of all viral proteins is shut down [4]. In immunocompromised hosts, however, EBV-infected B lymphoblasts can proliferate to cause lymphoproliferative disorder [1]. Thus, EBV persistence in human hosts is based on a fine balance between the host immunosurveillance, especially the function of EBV-specific cytotoxic T lymphocytes, and the replicative potential of EBV and the growth potential of EBV-infected cells.

Recently, we developed a new humanized mouse model of EBV infection, based on the NOD/Shi-*scid*/interleukin-2Rγ^{null} (NOG) mouse strain [5], that can reproduce key aspects of human EBV infection, such as lymphoproliferative disorder, asymptomatic persistent infection, and humoral and T cell–mediated immune responses [6]. In this model, inoculation with high-dose EBV ($\sim 1 \times 10^3$ 50% transformation dose [TD_{50}]) resulted in the development of lymphoproliferative disorder, whereas inoculation with low-dose virus ($\leq 1 \times 10^1$ TD_{50}) tended to cause apparently asymptomatic persistent infection. Enzyme-linked immunospot assay and flow cytometry identified CD8$^+$ T cells that recognize autologous EBV-transformed lymphoblastoid cells and produce IFN-γ in a human major histocompatibility complex class I–restricted manner [6]. Although immune responses to EBV have been demonstrated in this NOG mouse model and other types of humanized mice [7, 8], whether these immune responses work functionally to control EBV infection has not been clarified. To address this issue, we examined whether T cells in humanized NOG mice have any influence on the survival of EBV-infected mice. We also tested whether CD8$^+$ T cells isolated from EBV-infected NOG mice have a capacity to suppress EBV-induced lymphocyte transformation.

Methods. NOG mice were obtained from the Central Institute for Experimental Animals, and cord blood samples were supplied by the Tokyo Cord Blood Bank after obtaining informed consent. Reconstitution of human immune system components was performed as described elsewhere [6, 9, 10]. In brief, CD34$^+$ human hematopoietic stem cells (HSCs) were isolated from cord blood with use of the MACS Direct CD34 Progenitor Cell Isolation Kit (Miltenyi Biotec), and 1×10^4–

Received 14 May 2009; accepted 19 June 2009; electronically published 15 October 2009.
Potential conflicts of interest: none reported.
Financial support: Ministry of Health, Labour and Welfare of Japan (H19-AIDS-003 and H21-AIDS-008) and a grant for the Research on Publicly Essential Drugs and Medical Devices from The Japan Health Sciences Foundation.
Reprints or correspondence: Dr. Shigeyoshi Fujiwara, Dept. of Infectious Diseases, National Research Institute for Child Health and Development, 2-10-1 Okura, Setagaya-ku, Tokyo 157-8535, Japan (shige@nch.go.jp).

The Journal of Infectious Diseases 2009;200:1611–15

0022-1899/2009/20010-0018$15.00
DOI: 10.1086/644644

1.2×10^5 cells/mouse of HSCs were transplanted in 6–10-week-old female NOG mice via the tail vein. The development of human blood cells in the peripheral blood was monitored by staining with monoclonal antibodies specific to human CD45RA, CD45RO, CD19, CD3, CD4, and CD8. NOG mice in which the human hematoimmune system was reconstituted are referred to here as humanized NOG mice. The term "lot" signifies a group of humanized mice derived from a single cord blood donor. Protocols of experiments with NOG mice were approved by the Institutional Animal Care and Use Committee of the National Institute of Infectious Diseases. The use of human materials in this research was approved by the In-

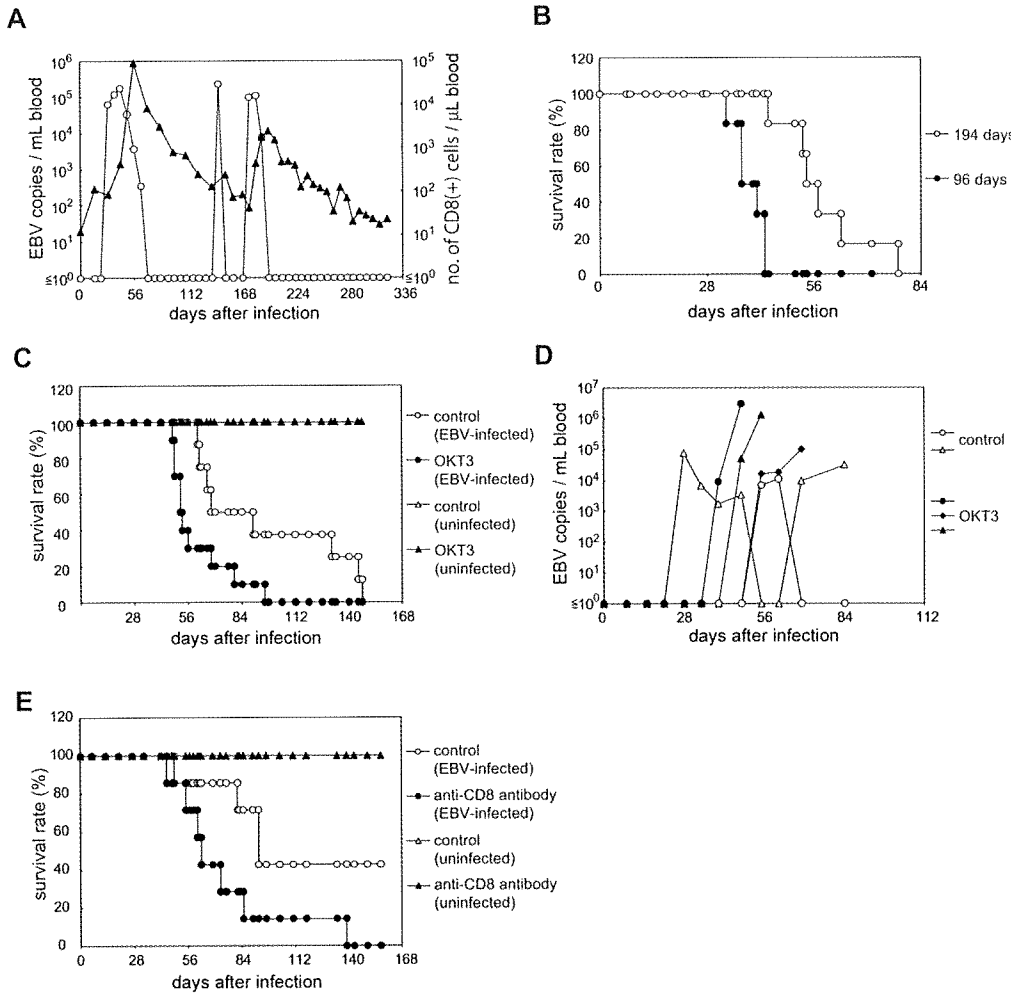

Figure 1. Evidence for T cell–mediated control of Epstein-Barr virus (EBV) infection in humanized NOD/Shi-*scid*/interleukin-2Rγ^{null} (NOG) mice. *A,* Associated changes in the number of $CD8^+$ T cells and viral DNA level in the peripheral blood of an EBV-infected humanized NOG mouse inoculated with EBV at ten 50% transformation dose (TD_{50}). The levels of EBV DNA *(open circles)* and $CD8^+$ T cells *(black triangles)* were monitored periodically. *B,* Survival curves of humanized NOG mice inoculated with EBV at different stages of reconstitution with human lymphocytes. Black circles represent mice inoculated with EBV (1×10^3 TD_{50}) at 96 days after transplantation with hematopoietic stem cells, and open circles represent mice inoculated at 194 days. *C,* Effect of depletion of T cells on the survival of EBV-infected humanized NOG mice. Black circles represent mice given daily intravenous injection with the OKT3 antibody (2 μg/mouse/day), starting at 21 days after infection, and open circles represent mice not given the antibody. Black triangles represent EBV-uninfected humanized NOG mice given OKT3 antibody, and open triangles represent such mice not given the antibody. *D,* Effect of depletion of T cells on the peripheral blood level of EBV DNA in humanized NOG mice. Black circles, black triangles, and black diamonds represent 3 humanized NOG mice inoculated with EBV (1×10^3 TD_{50}) that were treated with OKT3 as described in *C,* and open circles and open triangles represent such mice not treated with the antibody. Interruption of records indicates the death of a mouse. *E,* Effect of antibody specific to the CD8 molecule (B9.11) on the survival of EBV-infected humanized NOG mice. Black circles represent EBV-infected humanized NOG mice given daily intravenous injection with B9.11 (2 μg/mouse/day), starting at 21 days after infection, and open circles represent such mice not given the injection. Black triangles represent humanized NOG mice not infected with EBV that were given OKT3 antibody, and open triangles represent such mice not given the antibody.

stitutional Review Boards of the National Research Institute for Child Health and Development, the National Institute of Infectious Diseases, and the Tokyo Cord Blood Bank.

Preparation of EBV inocula and their titration, intravenous inoculation to humanized NOG mice, and quantification of viral DNA were performed as described elsewhere [6]. In brief, virus production from Akata cells was stimulated by treatment with anti-IgG antibody (DAKO), and culture fluid was used as inoculum after filtration through a 0.45-μm membrane filter. EBV titers in TD_{50} were determined by the Reed-Muench method.

In T cell reduction experiments, humanized NOG mice were inoculated with EBV at a dose of 1×10^2 TD_{50}. Starting at 21 days after inoculation, the Orthoclone OKT3 antibody specific to CD3 (Janssen Pharmaceutical) or the B9.11 antibody specific to CD8 (Beckman-Coulter) was administered intravenously at a dosage of 2 μg/mouse/day everyday until the end of the experiment. In a typical mouse treated with OKT3, 0.1% of human $CD45^+$ cells were $CD4^+CD8^-$ and 0.8% were $CD4^-CD8^+$ 2 weeks after the initiation of OKT3 administration, whereas in a control mouse, 15.0% of human $CD45^+$ cells were $CD4^+CD8^-$ and 12.5% were $CD4^-CD8^+$. Thus, this antibody was effective in significantly reducing the number of specific target cells. Confirmation of the reduction of $CD8^+$ cells by B9.11 was not possible, because this antibody covered the epitope recognized by antibodies available for flow cytometry. Survival curves of antibody-treated and untreated mice were compared statistically by the log-rank test.

Direct suppression of EBV-induced B cell transformation by $CD8^+$ T cells was assessed by the transformation regression assay based on a previously described method [11, 12]. $CD8^+$ T cells were isolated, as described elsewhere [6], from the spleen of EBV-infected or uninfected humanized NOG mice. Mononuclear cells were isolated from the spleen of uninfected humanized NOG mice and were inoculated with EBV (3×10^3 TD_{50} per 1×10^7 splenocytes). These EBV-infected cells were dispensed into microplates (3×10^4–1×10^5 cells/well) and were mixed with $CD8^+$ T cells in the wells of microculture plates at different ratios. Half of the medium was replaced with fresh medium each week, and the outgrowth of lymphoblastoid cell lines was counted 8 weeks after initiation of the culture. Humanized NOG mice in the same lot were used in each experiment to attain common background of human major histocompatibility complex. The number of $CD8^+$ T cells required to achieve regression in 50% of the wells (50% regression dose) was calculated by the Reed-Muench method.

Results. Our previous experiments indicated that EBV-infected humanized NOG mice mount an EBV-specific T cell response that may be involved in immunological control of EBV. A time course of the levels of EBV DNA and $CD8^+$ T cells in the peripheral blood of a representative EBV-infected mouse (Figure 1*A*) suggested that these parameters change in an associated manner; there was a tendency for $CD8^+$ T cells to increase after surges in the EBV DNA level and to gradually decrease as the EBV DNA level decreased, suggesting that these $CD8^+$ T cells have some role in the control of EBV DNA level.

Table 1. Fifty Percent Regression Dose of $CD8^+$ T Cells in Epstein-Barr Virus (EBV)–Infected and Uninfected Mice

	50% Regression dose	
Experiment[a]	EBV-infected mice	Uninfected mice
A1	2.7×10^4	$>9.9 \times 10^4$
B1-1	2.7×10^5	$>1.4 \times 10^6$
B1-2	2.4×10^5	$>8.5 \times 10^5$
B2	1.1×10^5	$>4.2 \times 10^5$
B3[b]	$>2.3 \times 10^5$	$>3.0 \times 10^5$
C1[b]	$>3.9 \times 10^5$	$>3.2 \times 10^5$
C2	2.0×10^4	$>1.7 \times 10^5$

[a] Alphabetical letters signify the lot of a mouse, and the number immediately after the letter indicates an individual mouse. Numbers after a hyphen identify individual experiments.
[b] No significant regression was seen in these experiments.

To examine the protective role of T cells more precisely, we next tested whether the development of T cells has any influence on the mice's resistance to EBV infection. After transplantation with human HSCs, B cells develop first, ~3 months after transplantation, and T cells differentiate later, ~6 months after transplantation [10]. We divided 12 humanized NOG mice in a lot into 2 groups; 6 mice were inoculated with EBV (1×10^3 TD_{50}) at 96 days after transplantation with HSCs, and the remaining 6 were inoculated at 194 days. Mice were examined daily, and those exhibiting signs of severe illness, including weight loss, piloerection, and cachexia, were sacrificed for analysis. On autopsy, most of these mice showed the signs of lymphoproliferative disorder, as described elsewhere [6]. Figure 1*B* shows the survival curve of each group of infected mice, and the log-rank test indicated that the mice inoculated at 6 months after transplantation (ie, with fully developed T cells) had a significantly elongated life span ($P < .001$).

Because the aforementioned results suggested that T lymphocytes reconstituted in humanized NOG mice have some role in the protection against EBV-induced lymphoproliferative disorder, we then examined the effect of the anti-CD3 monoclonal antibody OKT3, which can deplete T cells in vivo [13]. Eighteen humanized NOG mice inoculated with 1×10^2 TD_{50} EBV were divided into 2 groups; 10 mice were given OKT3 beginning at 21 days after inoculation, and the remaining 8 were not given the antibody. Figure 1*C* shows the survival curve of these mice. The log-rank test indicated that those mice treated with OKT3 antibody had a significantly shorter life span, compared with control mice ($P < .01$). Similar OKT3 treatment

was performed with 7 humanized NOG mice that were not infected with EBV; 4 mice were given OKT3 antibody, and 3 were not. The result indicated that all mice in both groups survived the observation period of 150 days, and no difference could be seen between them, excluding the possibility that OKT3 has its own toxicity (Figure 1*C*). In accordance with this result, quantification with real-time polymerase chain reaction indicated that the level of EBV DNA in the peripheral blood was consistently higher in the OKT3-treated mice than in control mice (Figure 1*D*). Because $CD8^+$ cytotoxic T cells are considered to play a central role in the immune response to EBV, we next examined the effect of an antibody (B9.11) specific to the CD8 molecule [14]. Figure 1*E* shows the survival curves of EBV-infected humanized NOG mice that were either treated with B9.11 or not, and the log-rank test indicated that those mice treated with the antibody had a significantly reduced life span after EBV infection ($P < .05$).

To test whether T cells isolated from EBV-infected mice have the ability to suppress transformation of autologous B cells by EBV, we used the transformation regression assay. Mononuclear cells isolated from the spleen of humanized NOG mice were inoculated with EBV and were cocultured with $CD8^+$ T cells isolated from the spleen of either EBV-infected or uninfected mice. Table 1 shows the number of $CD8^+$ T cells required to inhibit the outgrowth of EBV-infected cells in 50% of the wells (50% regression dose). These data indicate that $CD8^+$ T cells isolated from EBV-infected mice, but not those from uninfected mice, could suppress the outgrowth of transformed lymphoblastoid cell line.

Discussion. Humanized mouse technology has been successfully used to reproduce human immune responses to certain viruses that cannot infect ordinary mice [6–8, 10]. However, these studies have yet to provide evidence that immune responses induced in these mice are actually involved in the control of viral infections. This was an important issue when we considered the possibility of using humanized mice as a tool to evaluate immunological therapies and prophylaxes to viral infections.

Humanized NOG mice in later stages of reconstitution that contained high numbers of T cells had significantly longer life spans after EBV infection, compared with those in earlier stages that lacked significant differentiation of T cells. In accordance with this result, treatment of EBV-infected humanized NOG mice with OKT3, which can deplete $CD3^+$ T cells, significantly reduced their life span. Furthermore, similar antibody-mediated reduction in the number of $CD8^+$ T cells also reduced the life span of infected humanized NOG mice. Thus, our results strongly suggest that human T cells that develop in humanized NOG mice contribute to their resistance to EBV infection. More-direct evidence of immunological control of EBV infection was obtained by the transformation regression assay, which has been used as one of the most reliable methods to quantify EBV-specific cytotoxic T cells. This assay clearly indicated that $CD8^+$ T cells isolated from EBV-infected mice can suppress EBV-induced transformation of autologous B cells. A study is underway to identify an epitope that can be recognized by a $CD8^+$ T cell clone.

To our knowledge, these results are the first evidence that immune responses induced in humanized mice are actually involved in an effective control of viral infection. It is thus suggested that the NOG mouse model of EBV infection is a useful tool to evaluate candidate vaccines and immunological therapies for EBV infection.

After the initial submission of this report, Strowig and others published a work containing similar findings, namely higher EBV load and lymphoproliferative disorder in humanized mice after T cell depletion [15].

Acknowledgments

We thank Motohiko Okano, for advice in regression assay; Miki Mizukami, Ken Watanabe, and Miki Katayama, for technical assistance; Yuko Tatsumi and Tomomi Hakuya, for secretarial assistance; and Tokyo Cord Blood Bank, for supplying cord blood.

References

1. Rickinson AB, Kieff E. Epstein-Barr virus. In: Knipe DM, Howley PM, eds. Fields virology. 5th ed. Vol. 2. Philadelphia: Lippincott Williams & Wilkins, **2007**:2655–700.
2. Kieff E, Rickinson AB. Epstein-Barr virus and its replication. In: Knipe DM, ed. Fields virology. 5th. ed. Vol. 2. Philadelphia: Lippincott Williams & Wilkins, **2007**:2603–54.
3. Hislop AD, Taylor GS, Sauce D, Rickinson AB. Cellular responses to viral infection in humans: lessons from Epstein-Barr virus. Annu Rev Immunol **2007**; 25:587–617.
4. Babcock GJ, Decker LL, Volk M, Thorley-Lawson DA. EBV persistence in memory B cells in vivo. Immunity **1998**; 9:395–404.
5. Ito M, Hiramatsu H, Kobayashi K, et al. NOD/SCID/gamma(c)(null) mouse: an excellent recipient mouse model for engraftment of human cells. Blood **2002**; 100:3175–82.
6. Yajima M, Imadome KI, Nakagawa A, et al. A new humanized mouse model of Epstein-Barr virus infection that reproduces persistent infection, lymphoproliferative disorder, and cell-mediated and humoral immune responses. J Infect Dis **2008**; 198:673–82.
7. Melkus MW, Estes JD, Padgett-Thomas A, et al. Humanized mice mount specific adaptive and innate immune responses to EBV and TSST-1. Nat Med **2006**; 12:1316–22.
8. Traggiai E, Chicha L, Mazzucchelli L, et al. Development of a human adaptive immune system in cord blood cell-transplanted mice. Science **2004**; 304:104–7.
9. Watanabe S, Ohta S, Yajima M, et al. Humanized NOD/SCID/IL2Rgamma(null) mice transplanted with hematopoietic stem cells under nonmyeloablative condition show prolonged lifespans and allow detailed analysis of human immunodeficiency virus type 1 pathogenesis. J Virol **2007**; 81:13259–64.
10. Watanabe S, Terashima K, Ohta S, et al. Hematopoietic stem cell-engrafted NOD/SCID/IL2Rgamma null mice develop human lymphoid

systems and induce long-lasting HIV-1 infection with specific humoral immune responses. Blood **2007**; 109:212–8.
11. Moss DJ, Rickinson AB, Pope JH. Long-term T-cell-mediated immunity to Epstein-Barr virus in man. I. Complete regression of virus-induced transformation in cultures of seropositive donor leukocytes. Int J Cancer **1978**; 22:662–8.
12. Okano M, Purtilo DT. Simple assay for evaluation of Epstein-Barr virus specific cytotoxic T lymphocytes. J Immunol Methods **1995**; 184:149–52.
13. Dessureault S, Shpitz B, Alloo J, et al. Physiologic human T-cell responses to OKT3 in the human peripheral blood lymphocyte-severe combined immunodeficiency mouse model. Transplantation **1997**; 64: 811–6.
14. Kobayashi E, Kawai K, Ikarashi Y, Fujiwara M. Mechanism of the rejection of major histocompatibility complex class I-disparate murine skin grafts: rejection can be mediated by CD4+ cells activated by allo-class I + II antigen in CD8+ cell-depleted hosts. J Exp Med **1992**; 176: 617–21.
15. Strowig T, Gurer C, Ploss A, et al. Priming of protective T cell responses against virus-induced tumors in mice with human immune system components. J Exp Med **2009**; 206:1423–34.

Int J Hematol (2008) 88:476–482
DOI 10.1007/s12185-008-0215-z

RAPID COMMUNICATION

Early development of human hematopoietic and acquired immune systems in new born NOD/Scid/Jak3^{null} mice intrahepatic engrafted with cord blood-derived CD34^{+} cells

Seiji Okada · Hideki Harada · Takaaki Ito · Takashi Saito · Shinya Suzu

Received: 17 June 2008 / Revised: 28 October 2008 / Accepted: 4 November 2008 / Published online: 28 November 2008

Abstract An animal model in which the human immune system can be reconstituted is necessary to study acquired immunity in vivo. We report here a novel model, the NOD/SCID/JAK3^{null} mouse, for the human immune system's development. Newborn mice transplanted with human cord blood CD34^{+} cells intrahepatically, developed human T and B cells, and myeloid and plasmacytoid dendritic cells. The T and B cells had a naïve to memory phenotype, and included plasma cells. The human acquired immune system can be reconstituted from CD34^{+} cells in NOD/SCID/JAK3^{null} mice. This model is a powerful tool for the study of human immunity.

Keywords Hematopoietic stem cell · Immunodeficient mice · CD34 · Transplantation1

1 Introduction

Xenotransplantation of human cells into immunocompromised mice has become an invaluable tool for studying the function of the human hematopoietic and immune systems [1, 2]. NOD/SCID mice have been widely used for the evaluation of human hematopoietic stem cell activity, because they exhibit deficiencies in NK cell activity, macrophage and DC function, and complement activation as well as T and B cell deficiencies. Recent advances have revealed that the complete abolishment of NK cell activity by anti-NK antibody treatment or intercrossing with NK defective genetically modified mice results in a high degree of engraftment with human hematopoietic cells and T cell development. Notably, recently established NOD/SCID/common γ chain knockout ($\gamma c^{-/-}$) and Balb/C-Rag-2$^{-/-}\gamma c^{-/-}$ mice offered superior engraftment capacity [3–5].

JAK3, a tyrosine kinase crucial for mediating signaling from the common γ-chain of cytokine receptors, is limited to cells that actively participate in the immune response to allografts [6]. Recent tests in stringent preclinical studies suggest that JAK3 inhibitiors are effective in preventing of allograft rejection with a narrow side-effect profile [7]. On the basis of these findings, NOD/SCID were crossed with JAK3^{null} mice [8] to produce a novel strain, NOD/SCID/JAK3^{null}, resulting in a complete lack of T, B, NK, and NKT cell function. We successfully reproduced myelo-lymphoid maturation by injecting human cord blood-derived CD34^{+} cells into the liver of newborn NOD/SCID/JAK3^{null} mice. Our data show that the NOD/SCID/JAK3^{null} newborn system provides a valuable tool with which to reproduce human hemato-lymphoid development.

Electronic supplementary material The online version of this article (doi:10.1007/s12185-008-0215-z) contains supplementary material, which is available to authorized users.

S. Okada (✉) · H. Harada · S. Suzu
Division of Hematopoiesis, Center for AIDS Research, Kumamoto University, 2-2-1, Honjo, Kumamoto 860-0811, Japan
e-mail: okadas@kumamoto-u.ac.jp

T. Ito
Department of Pathology and Experimental Medicine, Graduate School of Medical Sciences, Kumamoto University, Kumamoto, Japan

T. Saito
Laboratory for Cell Signaling, RIKEN Research Center for Allergy and Immunology, Yokohama 230-0045, Japan

2 Materials and methods

2.1 Mice

The NOD/SCID/JAK3^{null} strain was established by backcrossing JAK3 ^{null} mice [8] with the NOD.Cg-Prkdc^{scid} strain for 10 generations. All experiments were performed according to the guidelines of the Institutional Animal Committee of Kumamoto University.

2.2 Cell preparation and transplantation

Umbilical cord blood cells were collected during normal full-term deliveries after obtaining informed consent, according to institutional guidelines approved by The Faculty of Medical and Pharmaceutical Sciences, Kumamoto University. CD34$^+$ cells were isolated using the CD34 Progenitor Cell Isolation Kit (Miltenyi Biotec, Sunnyvale, CA). The purity of the CD34$^+$ cells after isolation was >90%, and contamination of CD3$^+$ cells was less than 5%. The CD34$^+$ cells (5×10^4) were transplanted into the liver of irradiated (1.2 Gy) newborn mice.

2.3 Flow cytometry

Mouse spleen cells were stained with DX5-FITC (pan NK marker), mCD122 (IL-2Rβ)-PE, mCD19-APC and mCD3-PE/Cy7 (eBiosciences, San Diego, CA) to detect the murine lymphocytes. Eight to sixteen wks after transplantation, peripheral blood samples were obtained from the retroorbital sinus. At the time of sacrifice, the thymus, the spleen and BM were collected, stained with mAbs for differentiation antigens, and analyzed using LSR II (BD Biosciences, San Jose, CA). The mAbs used were human (h) CD3-APC, hCD4-FITC, hCD11c-APC, hCD33-FITC, hCD34-PE, hCD45-FITC, and mCD45.1-PE (BD Biosciences, San Diego, CA), hCD3-PE/Cy7, hCD20-PE, hCD38-PE, hCD56-PE, hCD123-PE, and hCD138-FITC (eBiosciences), hCD8-PB, hCCR7-PE, hCD19-PB, hCD27-APC, and hCD45-PB (Dako Cytomation, Glostrup, Denmark), BDCA-1(CD1c)-PE, BDCA-2(CD303)-FITC, BDCA-3(CD141)-FITC (Miltenyi Biotech), IgD-FITC (Sigma, St. Louis, MO), and hCD45RA-ECD (Beckman Coulter, Fullerton, CA). Data were analyzed with FlowJo (Tree Star, San Carlos, CA).

2.4 Cytotoxicity assay

The cytotoxic activity of the murine NK cells was measured by flowcytometry-based cytotoxicity assay with CFSE-labeled Yac-1 cells and propidium iodide (PI) as described by Marcusson-Stahl et al. [9, 10]. Briefly, target Yac-1 cells were stained with 2 μM of fluorescence labeling reagent, 5-(6)-carboxy-fluorescein succinimidyl ester (CFSE, Molecular Probes, OR) as described in manufacturer's instruction. Fifty μl aliquots of CFSE-labeled Yac-1 cells (1×10^5cell/ml) were placed in 5-ml round-bottomed tubes, and 400 μl of twofold serial diluted mononuclear cells from spleen was added into the tubes as effector cells. Effector or target cells alone were used as negative controls. After 4 h incubation at 37°C, 50 μl of 20 μg/ml PI was added and cells were incubated for an additional 15 min. Target cells in FSC (forward scatter) versus SSC (side scatter) dot plots were gated, and CFSE and PI were measured by LSR II flowcytometer. Cytotoxic activity was calculated as follows: $A/(A + B) \times 100 - C$ (%), where A is the percentage of PI^+EGFP^+ cells; B is the percentage of PI^-GFP^+ cells at each E/T ratio; C is the percentage of spontaneous PI^+ cells without effector cells ($A/(A + B) \times 100$ (%) at E/T ratio = 0).

2.5 Histologic analysis

Tissue samples were fixed with 10% neutral-buffered formalin embedded in paraffin, cut into 4-μm sections, and immunostained with mouse anti-CD19, anti-CD3, and antiCD4 antibodies (Dako Cytomation, Carpinteria, CA). After rinsing, the sections were incubated with goat anti-mouse-Ig horseradish peroxidase complex (Nichirei, Tokyo, Japan) for 30 min and visualized with the use of 3,3′-diaminobenzidine (DAKO, Glostrup, Denmark) in 0.05 M acetate buffer containing 0.015% H_2O_2.

2.6 Proliferative responses to PHA and human IL-2

Spleen cells of englafted mice were aseptically prepared as single-cell suspension. The cells were cultured in RPMI-1690 containing 20% human AB plasma with PHA (1 μg/ml) or human IL-2 (200U/ml. Peprotech,Rocky Hill, NJ) at 3×10^5 cells/100 μl in microtiter plate. After incubation for 4 days, Tetrazolium dye methylthiotetrazole (MTT, 0.5 mg/ml final conc.) (Sigma) was added to each well. After 3 h of additional incubation, 100 μl of a solution containing 10% SDS plus 0.01 N HCl was added to dissolve the crystal. The absorption values at 570 nm were determined with an automatic ELISA plate reader (Multiskan, Thermo ElectronVantaa, Finland).

3 Results and discussion

3.1 Development of severe immunodeficient NOD/SCID/JAK3^{null} mice

The NOD/SCID/JAK3^{null} mice were established by backcrossing C57BL/6-JAK3^{null} mice [8] with NOD/SCID

mice for ten generations. Flow cytometric analysis a complete absence of $CD3^+$ T cells and NKT cells, $CD19^+$ B cells, and $DX5^+CD122(IL\text{-}2R\beta)^+$ NK cells in the spleen (Fig. 1a). NK cell activity was also hardly detectable in NOD/SCID/JAK3^{null} mice in functional examinations (Fig. 1b). NOD strain is known to have functional defects for macrophages and dendritic cells, and compliment deficiency [1, 2]. Thus, NOD/SCID/JAK3^{null} mice have severely impaired immunologic function.

3.2 Early T cell reconstitution in NOD/SCID/JAK3^{null} mice

To establish the human hemolymphoid system, newborn NOD/SCID/JAK3^{null} mice were transplanted intrahepatically with 5×10^4 $CD34^+$ CB cells. Peripheral blood was collected at various intervals for up to 16 wks, and analyzed by flow cytometry for the presence of human cells expressing the common human leukocyte antigen CD45 and the T lineage marker CD3. Seven wks after transplantation, human $CD45^+$ cells were already detected ($53.6 \pm 16.2\%$) (Fig. 2a, b), though most of them were $CD19^+$ B lymphocytes (data not shown), and only a few $CD45^+CD3^+$ T lymphocytes ($1.2 \pm 0.4\%$ of $hCD45^+$ cells) were observed. However, human T lymphocytes began to emerge and proliferate after 12 weeks and made up to $62.8 \pm 19.5\%$ of the $CD45^+$ cells at 16 wks. Representative profiles of $CD3^+$ cell kinetics from the same individual NOD/SCID/JAK3^{null} mice are shown in Fig. 2b. The reconstitution of T cells occurred earlier in the in NOD/SCID/JAK3^{null} newborn system than in the adult recipient system, where it usually takes more than 13 weeks [3].

3.3 Human acquired immune system reconstitution from $CD34^+$ cells in NOD/SCID/JAK3^{null} mice

At 16 weeks after transplantation, the thymus, the spleen and bone marrow were harvested and analyzed by flow cytometry. Myeloid differentiation from cord blood-derived hematopoietic stem cells was observed in the bone marrow of the transplanted NOD/SCID/JAK3^{null} mice,

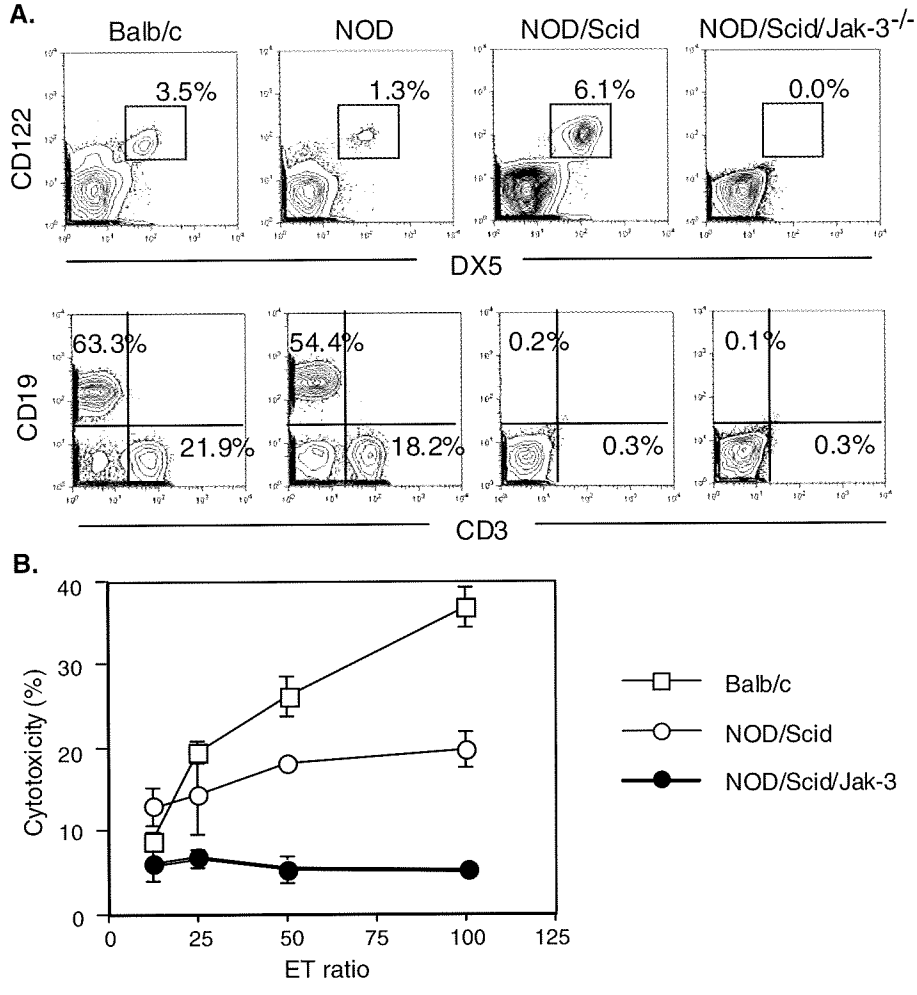

Fig. 1 Lymphocytes and NK cell activity in NOD/SCID/JAK3^{null} mice. **a** Spleen cells from mice were stained with DX5-FITC (pan NK marker), CD122(IL-2RB)-PE, CD19-APC and CD3-PE/Cy7. No NK T, and B cells were observed in the spleens of NOD/SCID/JAK3^{null} mice. **b** Absence of NK activity in NOD/SCID?JAK3^{null} mice. Spleen cells from Balb/c, NOD/SCID, and NOD/SCID/JAK3^{null} mice were used. The formula for percentage cytotoxicity is described in Sect. 2. Each value represents the mean of data from four mice

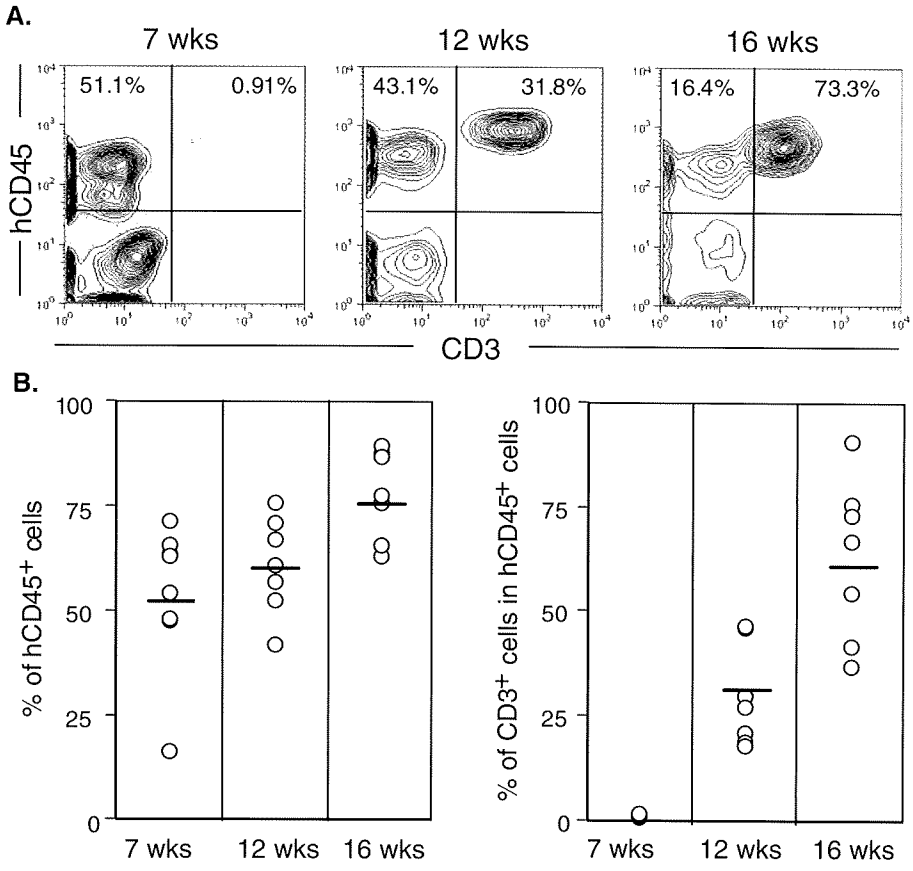

Fig. 2 Reconstitution of human T lymphocytes in $CD34^+$ cell-engrafted NOD/SCID/$JAK3^{null}$ recipients. **a** Kinetics of human cells in NOD/SCID/$JAK3^{null}$ newborn mice (a litter, $n = 8$) transplanted with human cord blood $CD34^+$ cells. Peripheral blood cells were collected at various intervals from $CD34^+$ cell-transplanted mice and stained with anti-mouse CD45.1, and anti-human CD45, CD3, and CD19. The cells were then analyzed by flow cytometry. Human hematopoietic cells were distinguished from mouse cells by the expression of human CD45. $CD3^+$ cells among the human $CD45^+$ cells were considered as human T lymphocytes. **b** Representative profiles of $CD45^+CD3^+$ peripheral blood cells in an individual NOD/Scid/$Jak3^{null}$ newborn mouse transplanted with human cord blood $CD34^+$ cells. A representative results from 5 independent experiments

including $CD34^-CD33^+$ myeloid cells (Fig. 3a), $CD14^+$ monocytes (data not shown), and $CD34^+$ hematopoietic stem cells. Human $CD45^+$ cells comprised 64.2 ± 11.5% of the spleen cells of engrafted NOD/SCID/$JAK3^{null}$ mice. The human cells were mainly $CD19^+$ B cells and $CD3^+$ T cells with a few $CD56^+CD3^-$ NK cells and $CD56^+CD3^+$ NKT cells. To further characterize the T lymphocytes emerging in the NOD/SCID/$JAK3^{null}$ mice, cells harvested from thymus and spleen were analyzed for T cell markers. All thymi contained double-positive, as well as CD4 and CD8 single positive, T cells (Fig. 3c). Based on the expression of CD45RA and CCR7, both human $CD4^+$ and $CD8^+$ T cells can be classified as naïve ($CD45RA^+$ $CCR7^+$), central memory ($CD45RA^-CCR7^+$), effector memory ($CD45RA^-CCR7^-$), and terminally differentiated ($CD45RA^+CCR7^-$) cells with different homing and effector capacities [11, 12]. All these fractions were observed in the spleen of transplanted mice. These results demonstrate that human T cell progenitors derived from $CD34^+$ cells can proliferate and differentiate into mature T cells in the NOD/SCID/$JAK3^{null}$ thymic and splenic microenvironment.

As for the development of B cells, 77.8 ± 10.2% of human $CD45^+$ cells in the bone marrow were $CD19^+$ B cells. Both immature CD20-negative and mature CD20-positive $CD19^+$ B cells were detected in bone marrow of engrafted mice (Fig. 3d). In the secondary lymphoid tissue, CD38 and Ig-D have been useful in classifying important developmental stages in the pathway from naïve to memory B cells (Bm1-Bm5) [13]. All of these stages of B cells were detected in spleen of reconstituted mice. Moreover, $CD138^+CD38^+CD27^+$ plasma cells were detected in bone marrow and spleen, indicating that full B cell maturation occurred in reconstituted NOD/SCID/$JAK3^{null}$ mice. Human DCs can be divided into $CD11c^{high}$ myeloid DCs (MDC) and $CD123^+CD303^+$ plasmacytoid DCs [14]. $CD11c^{high}$ myeloid DCs are subdivided into MDC1 and MDC2 by the expression of CD1c and CD141. All three subsets were present in BM and spleen of reconstituted mice. Immunohistochemical staining for the expression of CD20, CD3, and CD4 showed that human lymphocytes in the spleen of reconstituted mice possessed follicular structures (Fig. 3f).

Next, we cultured the unseparated splenocytes with PHA or human IL-2. As shown in Fig. 4, splenocytes from these engrafted mice showed a vigous proliferative response to these T cell mitogens. Although we observed human T cell proliferation with mitogen or human IL-2, it is still unknown whether generated T cells have fully functional or not. Indeed, low or absent immune response

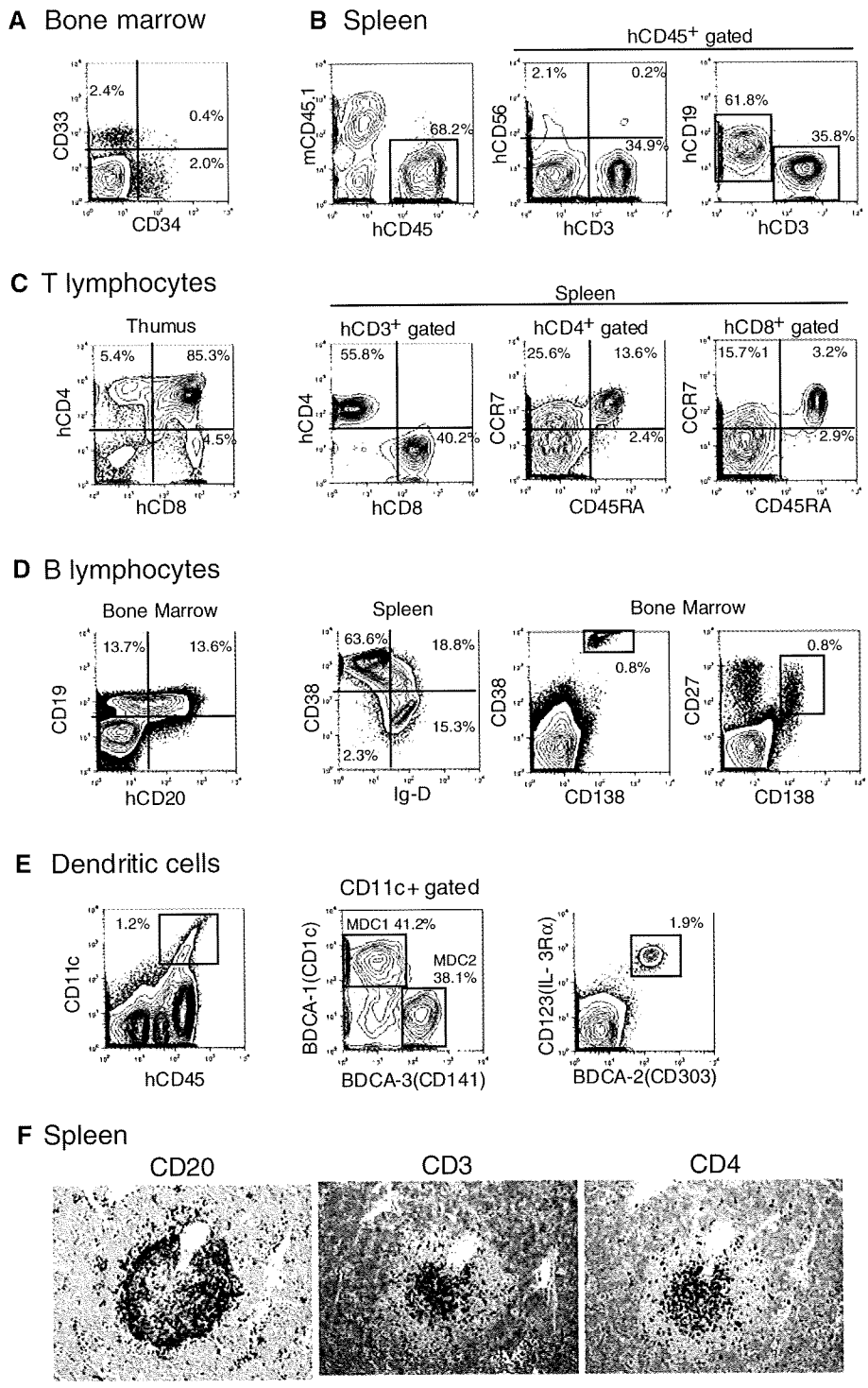

Fig. 3 Analysis of human hematopoietic cells in NOD/SCID/JAK3^{null} recipients. **a** Bone marrow contained CD33$^-$CD34$^+$ immature hematopoeitic stem cells and CD33$^+$ myeloid progenitors. **b** Spleen consisted of both human (hCD45$^+$) and murine (mCD45.1$^+$) white blood cells. Human white blood cells consisted of B cells(CD19$^+$), T cells (CD3$^+$), NK cells (CD3$^-$CD56$^+$) and NKT cells (CD3$^+$CD56$^-$). **c** The majority of cells in the thymus were CD4/CD8 double positive thymocytes. The CD3 + spleen cells included CD4$^+$ or CD8$^+$ single positive mature T cells. Both CD4$^+$ and CD8$^+$ T cells included naïve (CD45RA$^+$CCR7$^+$), central memory (CD45RA$^-$CCR7$^+$), effector memory (CD45RA$^-$CCR7$^-$), and terminally differentiated (CD45RA$^+$CCR7$^-$) cells. **d** Bone marrow contained CD19$^+$CD20$^-$ immature and CD19$^+$CD20$^+$ mature B cells. Naïve (CD19$^+$Ig-D$^+$CD38$^+$) to memory (CD19$^+$Ig-D$^-$CD38$^-$) B cell differentiation was observed in the spleen. CD138$^+$CD38$^+$CD27$^+$ plasma cells were detected in bone marrow. **e** BM contained hCD45$^+$CD11c$^+$ human DCs. CD11c+ DCs included CD1c$^+$ MDC1 and CD141$^+$ MDC2. BM also contained CD123/CD303 double positive human plasmacytoid DCs. **f** Immunohistochemistry of engrafted NOD/Scid/Jak3^{null} mouse spleen showed follicular structures in CD20$^+$ and CD3$^+$ human lymphocytes

were observed in HIV-1-exposed immunodeficeint mice transplanted with human CD34$^+$ cells [15–17], which is explained by insufficient MHC selection of human T cells in the mouse thymus and possible lack of some cross reactive cytokines and chemokines in the xenogenic environment [18]. This speculation is supported by the fact that co-transplantation of human fetal/liver tissues and human CD34$^+$ cells enabled the mice to induce the antigen-specific T-cell response and T cell dependent antibody production [19]. Detailed analysis and additional ingenuity is needed to induce the functional human immune response.

The Rag-2$^{-/-}\gamma c^{-/-}$ newborn, and NOD/SCID/$\gamma c^{-/-}$ adult and newborn models have already provided definitive

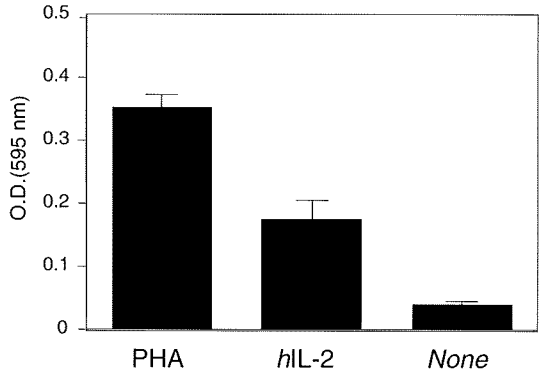

Fig. 4 Proliferative response of spleen cells from engrafted NOD/SCID/JAK3^{null} mice. Proliferative response of unfractionated splenocytes obtained from 16 weeks old NOD/SCID/JAK3^{null} mice. Data shown are mean ± SD of three mice

evidence that functional T cells, B cells, and DCs can develop from hematopoietic stem cells in immunodeficient mice [3–5], which is recently called "humanized mice" [1, 20]. Consistent with these previous models, the NOD/SCID/JAK3^{null} newborn model provided full T and B cell maturation as well as DC development. The engrafted mice looked healthy and there were no signs and symptoms of apparent xenogenic graft versus host disease (GVHD) until 6 months after birth, which is also consistent with previous models [3, 21]. Then the mice were gradually going to die after 6 months with unknown reason. Further histological examination is needed to clarify the cause of death including the late occurring GVHD or the influence of irradiation at the time of birth. There are two advantages to our NOD/SCID/JAK3^{null} newborn model. First, T cell ontogeny occurs earlier than in adult models. The full T cell reconstitution takes 12 weeks after birth in our model (Fig. 2), whereas adult models take 23 weeks (Transplantation into 7-week-old adult mice and reconstitution takes 16 weeks) [3]. This is extremely important for enabling long term experimentation because the life span of the NOD/SCID strain and irradiated mice is relatively short [22, 23]. Second, it is relatively easy to transplant the hematopoietic stem cells into newborn liver via the cutaneous rather than intravenous route [3, 5]. In addition, since relatively small number of CD34$^+$ cells (5×10^4/mouse) can reconstitute the human hematopoietic and immune system in the NOD/SCID/JAK3^{null} mice reproducibly, a single human stem cell donor can seed sufficient number of mice for testing novel therapeutic strategies such as proof-of-concept mechanistic models and models of human infectious disease.

In summary, we showed that the NOD/SCID/JAK3^{null} newborn system efficiently supports the development of human B and T lymphocytes from cord blood-derived CD34$^+$ cells, passing through physiological developmental intermediates, and the development of human dendritic cells. NOD/SCID/JAK3^{null} mice are a powerful and versatile tool that can be used to analyze the human hematopoietic and immune systems in response to infection, cancer, and drug regimens without putting patients at risk.

Acknowledgments We are grateful to Dr. K. Matsui and his coworkers (Fukuda Hospital, Kumamoto, Japan) for providing cord blood. We thank I. Suzu for technical assistance and Y. Endo for secretarial assistance. This work was supported in part by Health and Labour Sciences Research Grants from the Ministry of Health, Labour and Welfare of Japan (H-16-AIDS-003 and H19-AIDS-003), by grants from the Ministry of Education, Science, Sports, and Culture of Japan, and by a Grant from the Uehara Memorial Foundation.

References

1. Shultz DL, Ishikawa F, Greiner DL. Humanized mice in translational biomedical research. Nat Rev Immunol. 2007;7:118–30. doi:10.1038/nri2017.
2. Legrand N, Weijer K, Spits H. Experimental models to study development and function of the human immune system in vivo. J Immunol. 2006;176:2053–8.
3. Yahata T, Ando K, Nakamura Y, Ueyama Y, Shimamura K, Tamaoki N, et al. Functional human T lymphocyte development from cord blood CD34 + cells in Nonobese Diabetic/Shi-Scid, IL-2 receptor γ null mice. J Immunol. 2002;169:204–9.
4. Traggiai E, Chicha L, Mazzucchelli L, Bronz L, Piffaretti JC, Lanzavecchia A, et al. Development of a human adaptive immune system in cord blood cell-transplanted mice. Science. 2004;304:104–7. doi:10.1126/science.1093933.
5. Ishikawa F, Yasukawa M, Lyons B, Yoshida S, Miyamato T, Yoshimoto G, et al. Development of functional human blood and immune systems in NOD/SCID/IL2 receptor γ chain^{null} mice. Blood. 2005;106:1565–73. doi:10.1182/blood-2005-02-0516.
6. Suzuki K, Nakajima H, Saito Y, Saito T, Leonard WJ, Iwamoto I. Janus kinase 3 (Jak3) is essential for common cytokine receptor gamma chain (gamma(c))-dependent signaling: comparative analysis of gamma(c), Jak3, and gamma(c) and Jak3 double-deficient mice. Int Immunol. 2000;12:123–32. doi:10.1093/intimm/12.2.123.
7. Borie DC, O'Shea JJ, Changelian PS. JAK3 inhibition, a viable new modality of immunosuppression for solid organ transplants. Trends Mol Med. 2004;10:532–41. doi:10.1016/j.molmed.2004.09.007.
8. Park SY, Saijo K, Takahashi T, et al. Developmental defects of lymphoid cells in Jak3 kinase-deficient mice. Immunity. 1995;3:771–82. doi:10.1016/1074-7613(95)90066-7.
9. Marcusson-Stahl M, Cederbrant K. A flow-cytometric NK-cytotoxicity assay adapted for use in rat repeated dose toxicity studies. Toxicology. 2003;193:269–79. doi:10.1016/S0300-483X(03)00302-0.
10. Koga T, Harada H, Shi TS, Okada S, Suico MA, Shuto T, et al. Hyperthermia suppresses the cytotoxicity of NK cells via down-regulation of perforin/granzyme B expression. Biochem Biophys Res Commun. 2005;337:1319–23. doi:10.1016/j.bbrc.2005.09.184.
11. De Rosa SC, Herzenberg LA, Herzenberg LA, Roederer M. 11-color, 13-parameter flow cytometry: identification of human

naive T cells by phenotype, function, and T-cell receptor diversity. Nat Med. 2001;7:245–8. doi:10.1038/84701.
12. Schaerli P, Moser B. Chemokines: control of primary and memory T-cell traffic. Immunol Res. 2005;31:57–74. doi:10.1385/IR:31:1:57.
13. Bohnhorst JO, Bjorgan MB, Thoen JE, Navtig JB, Thompson KM. Bm1-Bm5 classification of peripheral blood B cells reveals circulating germinal center founder cells in healthy individuals and disturbance in the B cell subpopulations in patients with primary Sjogren's syndrome. J Immunol. 2001;167:3610–8.
14. Dzionek A, Fuchs A, Schmidt P, Cremer S, Zysk M, Miltenyi S, et al. BDCA-2, BDCA-3, and BDCA-4: three markers for distinct subsets of dendritic cells in human peripheral blood. J Immunol. 2000;165:6037–46.
15. Zhang L, Kovalev GI, Su L. HIV-1 infection and pathogenesis in a novel humanized mouse model. Blood. 2007;109:2978–81.
16. An DS, Poon B, Ho Tsong Fang R, Weijer K, Blom B, Spits H, et al. Use of a novel chimeric mouse model with a functionally active human immune system to study human immunodeficiency virus type 1 infection. Clin Vaccine Immunol. 2007;14:391–6. doi:10.1128/CVI.00403-06.
17. Watanabe S, Terashima K, Ohta S, Horibata S, Yajima M, Shiozawa Y, et al. Hematopoietic stem cell-engrafted NOD/SCID/IL2Rγ^{null} mice develop human lymphoid systems and induce long-lasting HIV-1 infection with specific humoral immune responses. Blood. 2007;109:212–8. doi:10.1182/blood-2006-04-017681.
18. Baenziger S, Tussiwand R, Schlaepfer E, Mazzucchelli L, Heikenwalder M, Kurrer MO, et al. Disseminated and sustained HIV infection in CD34$^+$ cord blood cell-transplanted Rag2$^{-/-}\gamma c^{-/-}$ mice. Proc Natl Acad Sci USA. 2006;103:15951–6. doi:10.1073/pnas.0604493103.
19. Tonomura N, Habiro K, Shimizu A, Sykes M, Yang YG. Antigen-specific human T-cell responses and T cell-dependent production of human antibodies in a humanized mouse model. Blood. 2008;111:4293–6. doi:10.1182/blood-2007-11-121319.
20. Macchiarini F, Manz MG, Palucka K, Shultz LD. Humanized mice: are we there yet? J Exp Med. 2005;202:1307–11. doi:10.1084/jem.20051547.
21. Shultz LD, Lyons BL, Burzenski LM, Gott B, Chen X, Chaleff S, et al. Human lymphoid and myeloid cell development in NOD/LtSz-scid IL2Rγ^{null} mice engrafted with mobilized human hemopoietic stem cells. J Immunol. 2005;174:6477–89.
22. Goldman JP, Blundell MP, Lopes L, Kinnon C, Di Santo JP, Thrasher AJ. Enhanced human cell engraftment in mice deficient in RAG2 and common cytokine receptor γ chain. Br J Haematol. 1998;103:335–42. doi:10.1046/j.1365-2141.1998.00980.x.
23. Watanabe S, Ohta S, Yajima M, Terashima K, Ito M, Mugishima H, et al. Humanized NOD/SCID/IL2Rγ^{null} mice transplanted with hematopoietic stem cells under nonmyeloablative conditions show prolonged life spans and allow detailed analysis of human immunodeficiency virus type 1 pathogenesis. J Virol. 2007;81:13259–64. doi:10.1128/JVI.01353-07.

Int. J. Cancer: **125,** 1464–1472 (2009)

Biscoclaurine alkaloid cepharanthine inhibits the growth of primary effusion lymphoma *in vitro* and *in vivo* and induces apoptosis *via* suppression of the NF-κB pathway

Naoko Takahashi-Makise[1], Shinya Suzu[1], Masateru Hiyoshi[1], Takeo Ohsugi[2], Harutaka Katano[3], Kazuo Umezawa[4] and Seiji Okada[1]*

[1]*Division of Hematopoiesis, Center for AIDS Research, Kumamoto University, Honjo, Kumamoto, Japan*
[2]*Division of Microbiology and Genetics, Center for Animal Resources and Development, Institute of Resource Development and Analysis, Kumamoto University, Honjo, Kumamoto, Japan*
[3]*Department of Pathology, National Institute of Infectious Diseases, Toyama, Shinjuku, Tokyo, Japan*
[4]*Department of Applied Chemistry, Faculty of Science and Technology, Keio University, Hiyoshi, Kohoku-Ku, Yokohama, Japan*

Primary effusion lymphoma (PEL) is a unique and recently identified non-Hodgkin's lymphoma that was originally identified in patients with AIDS. PEL is caused by the Kaposi sarcoma-associated herpes virus (KSHV/HHV-8) and shows a peculiar presentation involving liquid growth in the serous body cavity and a poor prognosis. As the nuclear factor (NF)-κB pathway is activated in PEL and plays a central role in oncogenesis, we examined the effect of a biscoclaurine alkaloid, cepharanthine (CEP) on PEL derived cell lines (BCBL-1, TY-1 and RM-P1), *in vitro* and *in vivo*. An methylthiotetrazole assay revealed that the cell proliferation of PEL cell lines was significantly suppressed by the addition of CEP (1–10 μg/ml). CEP also inhibited NF-κB activation and induced apoptotic cell death in PEL cell lines. We established a PEL animal model by intraperitoneal injection of BCBL-1, which led to the development of ascites and diffuse infiltration of organs, without obvious solid lymphoma formation, which resembles the diffuse nature of human PEL. Intraperitoneal administration of CEP inhibited ascites formation and diffuse infiltration of BCBL-1 without significant systemic toxicity in this model. These results indicate that NF-κB could be an ideal molecular target for treating PEL and that CEP is quite useful as a unique therapeutic agent for PEL.

Key words: NF-κB; primary effusion lymphoma; cepharanthine; animal model

Primary effusion lymphoma (PEL) is a subtype of non-Hodgkin's B cell lymphoma that mainly presents in patients with advanced AIDS, but is sometimes also found in immunosuppressed patients such as those who have undergo organ transplantation.[1,2] Among AIDS-related NHLs, PEL generally has an extremely aggressive clinical course with a median survival of only 3 months.[3] PEL usually presents as a lymphomatous effusion in body cavities and is caused by Kaposi sarcoma-associated herpes virus (KSVH/HHV-8).[1] A number of constitutively activated signaling pathways play critical roles in the survival and growth of PEL cells. These include nuclear factor (NF)-κB, JAK/STAT and PI3 kinase.[4–6] KSHV/HHV-8 encodes a virus Fas-associated death domain-like interleukin-1β-converting enzyme (FLICE) inhibitory protein (vFLIP) that has the ability to activate the NF-κB pathway.[7–9] vFLIP has been shown to bind to the IKK complex to induce constitutive kinase activation,[10] and as a result, PEL cells have high levels of nuclear NF-κB activity, whereas inhibition of NF-κB induces apoptosis in PEL cells.[5,11] These studies support the idea that vFLIP-mediated NF-κB activation is necessary for the survival of PEL cells and that this pathway represents a target for molecular therapy for this disease.

Cepharanthine (CEP) is a biscoclaurine (bisbenzylisoquinoline) amphipathic alkaloid that was isolated from *Stephania cepharantha* Hayata. CEP and extracts from this plant are widely used, primarily in Japan, to treat a variety of acute and chronic diseases without any serious side effects.[12] CEP is known to possess various biological and pharmacological activities, including membrane-stabilizing,[13,14] immunomodulatory,[15] and anti-inflammatory activities.[16] CEP also has antiproliferative and proapoptotic effects against a diverse range of tumors both *in vitro* and *in vivo*.[17–21] In addition, this agent has been shown to inhibit the activation of NF-κB,[22,23] a transcription factor of critical importance in the regulation of cell growth and survival.

In the present study, we investigated the antitumor activity of CEP against human PEL cell lines. CEP inhibits constitutive active NF-κB, leading to apoptosis in PEL. Our findings provide the experimental basis for utilizing CEP against tumors activated by NF-κB.

Material and methods

Cell lines and reagents

The human PEL cell lines, BCBL-1 (obtained through the AIDS Research and Reference Reagent Program, Division of AIDS, NIAID, NIH),[24] TY-1[25] and RM-P1 (a kind gift of Dr. T. Taira, University of the Ryukyus, Japan),[26] and non-PEL human B cell lines, BALL-1 (a kind gift of Dr. K. Kuwahara, Kumamoto University, Japan), RAMOS (a kind gift of Dr. K. Kuwahara, Kumamoto University, Japan) and Raji (obtained from RIKEN Cell Bank, Tsukuba, Japan) were maintained in RPMI1640 supplemented with 10% heat inactivated fetal calf serum, penicillin (100 U/ml) and streptomycin (100 μg/ml) in a humidified incubator at 37°C and 5% CO_2. CEP was kindly provided by Kaken Shoyaku Co., Ltd. (Tokyo, Japan). DHMEQ is a NF-κB inhibitor that acts at the level of nuclear translocation of NF-κB.[27]

Tetrazolium dye methylthiotetrazole assay

The antiproliferative effects of CEP against PEL and non-PEL B cell lines were measured by the methylthiotetrazole (MTT) method (Sigma, St. Louis, MO). Briefly, 2×10^4 cells were incubated in triplicate in a 96-well microculture plate in the presence of different concentrations of CEP in a final volume of 0.1 ml for 48 hr at 37°C. Subsequently, MTT (0.5 mg/ml final concentration) was added to each well. After 3 hr of additional incubation, 100 μl of a solution containing 10% SDS plus 0.01 N HCl were added to dissolve the crystal. The absorption values at 570 nm were determined with an automatic enzyme-linked immnosorbent assay (ELISA) plate reader (Multiskan, Thermo ElectronVantaa, Finland). Values are normalized to the untreated (control) samples.

Grant sponsor: Ministry of Health, Labour and Welfare of Japan; Grant number: H19-AIDS-003; Grant sponsor: Ministry of Education, Science, Sports, and Culture of Japan.
***Correspondence to:** Division of Hematopoiesis, Center for AIDS Research, Kumamoto University, 2-2-1 Honjo, Kumamoto, 860-0811, Japan. Fax: +81-96-373-6523. E-mail: okadas@kumamoto-u.ac.jp
Received 20 September 2008; Revised 31 March 2009; Accepted after revision 7 April 2009
DOI 10.1002/ijc.24521
Published online 23 April 2009 in Wiley InterScience (www.interscience.wiley.com).

Cell cycle analysis

For cell cycle analysis, after PEL cells were treated with CEP for18 hr, the cells were incubated in hypotonic lysing buffer [0.1% sodium citrate, 0.1% Triton X, 0.1% RNase A and 50 μg/ml propidium iodide (PI)] at 4°C for 4 hr.[28] DNA content in each cell was analyzed on LSR II flow cytometer (BD Bioscience, San Jose, CA). Data were analyzed on FlowJo software (Tree Star, San Carlos, CA).

Annexin V assay

Apoptosis was quantified using the Annexin V: PE apoptosis detection kit I (BD Biosciences). Briefly, after treatment with CEP, cells were harvested, washed and then incubated with Annexin V-PE and 7-AAD for 15 min in the dark, before being analyzed on a LSR II cytometer.

Caspase activity measurements with flowcytometry

The active caspase 3 activity was measured using PhiPhiLux-G2D2 (OncoImmunin, Gaithersburg, MD)[29] according to the manufacturer's instructions. Briefly, CEP treated or untreated cells were incubated with 10 μM caspase substrate for 60 min, added 2 μl/ml of PI and analyzed by LSR II. Data were analyzed on FlowJo software, expressed casepase 3 positive cellular events among PI-negative (living) cells.

Western blot analysis

BCBL-1, TY-1 and RM-P1 cells with or without treatment of 10 μg/ml of CEP for 24 hr were collected and washed in cold PBS before the addition of 400 μl of cold buffer A (10 mM HEPES-KOH pH 7.9, 1.5 mM $MgCl_2$, 10 mM KCl, 0.1% NP-40, 0.5 mM DTT, 0.5 mM PMSF, 2 μg/ml pepstatin A, 2 μg/ml aprotinin and 2 μg/ml leupeptin). After incubation on ice for 10 min, the samples were vortexed for 10 sec. Nuclei were pelleted by centrifugation at 5,000 rpm for 1 min and washed once with buffer A. Fifty microliters of buffer C (50 mM HEPES-KOH pH 7.9, 10% glycerol, 420 mM KCl, 5 mM $MgCl_2$, 0.1 mM EDTA, 1 mM DTT, 0.5 mM PMSF, 2 μg/ml pepstatin A, 2 μg/ml aprotinin and 2 μg/ml leupeptin) were added to the nuclei and incubated on ice for 30 min. Nuclear extracts were obtained by centrifugation at 15,000 rpm for 15 min, then the nuclear extracts (40 μg protein) were separated by 10% SDS-PAGE and blotted onto a PVDF membrane (GE Healthcare, Tokyo, Japan). Detection was performed using Enhanced Chemiluminescence Western Blotting Detection System (ECL, GE Healthcare Bio-Science, Buckinghamshire, UK). Primary antibodies used were as follows: anti-p65 (F-6), anti-phospho(Ser311)-p65, anti-IκBα(C-21), anti-phospho(Ser32)-IκBα (B-6), anti-IKKαβ (H-479), anti-phospho(Thr23)-IKKαβ, anti-Actin(C-2) and anti-Histone H1(N-16) (Santa CruZ Biotechnology, Santa Cruz, CA).

Quantification of the Western blots was performed using NIH Image software (NIH, Bethesda, MD). Relative density was evaluated and normalized with actin or Histone H1.

Measurement of nuclear active NF-κB p65

PEL cells are treated with CEP for 18 hr and nuclear active NF-κB p65 was measured using an ELISA according to the manufactures's protocol (IMGENEX, San Diego, CA). In brief, the cells were centrifuged at 400*g* for 1 min and washed with cold phosphate buffered saline (PBS). The cells were lyzed by 400 μl of hypotonic buffer and 30 μl of 10% NP-40 was added. The mixture was centrifuged at 18,000*g* for 30 sec. The pellet was resuspended in 220 μl of nuclear extraction buffer and centrifuged at 18,000*g* for 1 min. The supernatant was used as nuclear extract. The anti-p65 antibody coated plate captured nuclear or cytoplasmic free p65 of samples (0.5–1 mg/ml of protein) and the amount of bound p65 was detected by adding a secondary antibody followed by alkaline phosphatase-conjugated secondary antibody. The absorbance value for each well was determined at 405 nm by a microplate reader (Bio-Rad). The relative activity of NF-κB is expressed as a percentage measured in control cells that were not treated with CEP.[30,31]

Electrophoretic mobility shift assay

The nuclear extracts from BCBL-1 cells were prepared using NF-κB/p65 ActiveELISA (IMGENEX). BCBL-1 cells that had been treated with CEP for the indicated period were collected and washed with PBS before 1× hypotonic buffer (1 ml) was added and then they were incubated on ice for 15 min. Fifty microliters of 10% detergent solution were added to the samples, and nuclei were collected by centrifugation at 14,000 rpm for 30 sec. One hundred microliters of nuclear lysis buffer were added to the nuclei, which were then incubated on ice for 30 min. Nuclear extracts were obtained by centrifugation at 14,000 rpm for 10 min. An electrophoretic mobility shift assay (EMSA) was performed using a 2nd generation DIG Gel Shit Kit (Roche Diagnostics, Mannheim, Germany). Briefly, double-stranded oligonucleotide probes containing the mouse immunoglobulin kappa (Igκ) light-chain NF-κB consensus site were purchased from Promega (Madison, WI). The oligonucleotide was 3′ end-labeled with a digoxigenin-11-ddUTP. The nuclear extract (10 μg protein) from BCBL-1 cells was incubated with 1 μg of poly[d(I-C)], 0.1 μg of poly-L-lysine and DIG-labeled oligonucleotide in binding buffer [20 mM HEPES pH 7.6, 1 mM EDTA, 10 mM $(NH_4)_2SO_4$, 0.2% Tween 20 and 30 mM KCl] for 15 min at 25°C. After the incubation, 5× loading buffer (0.25× TBE and 60% glycerol) was added, and the samples were separated on 5% acrylamide gel in 0.5× TBE buffer. The oligonucleotide was electroblotted onto a positively charged nylon membrane (Roche Diagnostics, Mannheim, Germany) and immunodetected using anti-digoxigenin-AP.

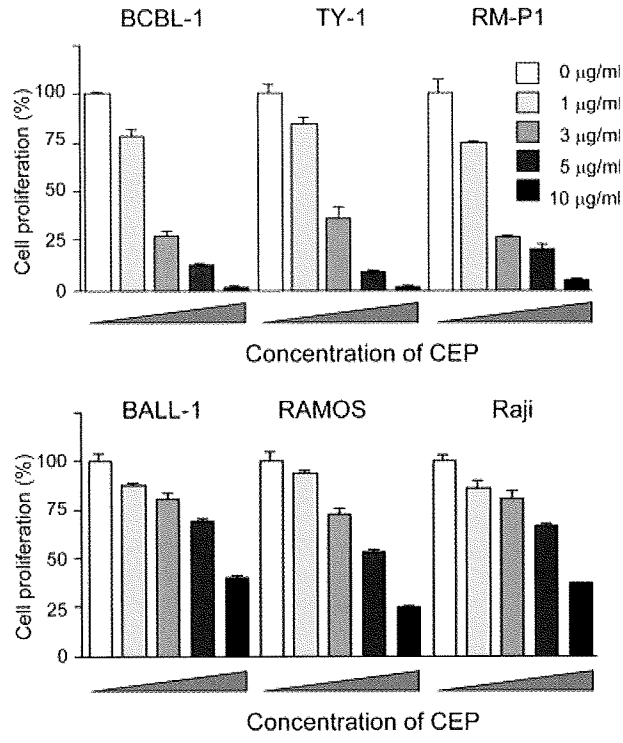

Figure 1 – CEP inhibits the proliferation of PEL cells. The PEL cell lines (BCBL-1, TY-1 and RM-P1) and non-PEL B cell lines (BALL-1, RAMOS and Raji) were incubated with 1, 3, 5, 10 μg/ml CEP for 48 hr. A cell proliferation assay was carried out using MTT as described in Material and methods section. One representative result from 3 independent experiments is shown.

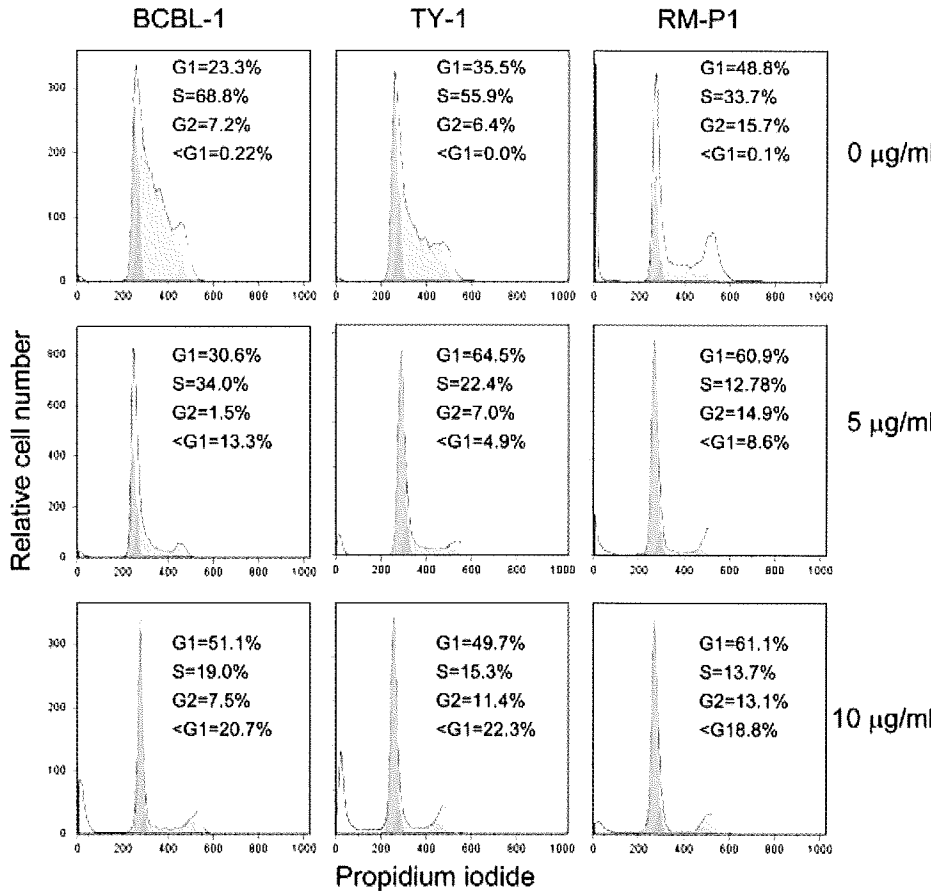

FIGURE 2 – CEP causes cell cycle arrest of PEL cells. The PEL cell lines BCBL-1, TY-1 and RM-P1 were treated with CEP (5 or 10 μg/ml) for 18 hr, and DNA histograms were determined and the cell cycle was analyzed using FlowJo software. One representative result from 3 independent experiments is shown. [Color figure can be viewed in the online issue, which is available at www.interscience.wiley.com.]

Xenograft mouse model

NOD/Scid/Jak3 deficient (NOJ) mice were established by backcrossing Jak3deficeint mice[32] with the NOD.Cg.-Prkdc^{scid} strain for 10 generations.[33] NOJ male mice 8-to 10-week-old were housed and monitored in our animal research facility according to the institutional guidelines. All experimental procedures and protocols were approved by the Institutional Animal Care and Use Committee at Kumamoto University. NOJ mice were intraperitoneally inoculated with 7×10^6 BCBL-1 cells suspended in 200 μl PBS. Then the mice were treated with intraperitoneal injections of PBS or CEP (10 mg/kg per day). Tumor burdens were evaluated by measuring the body weight and ascites.

Immunohistochemistry

To investigate the expression of KSHV/HHV-8 ORF73 (LANA) protein, tissue samples were fixed with 10% neutral-buffered formalin, embedded in paraffin and cut into 4-μm sections. The sections were deparaffinized by sequential immersion in xylene and ethanol and rehydrated in distilled water. They were then irradiated for 15 min in a microwave oven for antigen retrieval. Endogenous peroxidase activity was blocked by immersing the sections in methanol/0.6% H_2O_2 for 30 min at room temperature. Affinity-purified PA1-73N antibody,[34] diluted 1:3,000 in PBS/5% bovine serum albumin (BSA), was then applied, and the sections were incubated overnight at 4°C. After washing in PBS twice, the second and third reactions and the amplification procedure were performed using kits according to the manufacturer's instructions (catalyzed signal amplification system kit; DAKO, Copenhagen, Denmark). The signal was visualized using 0.2 mg/ml diaminobenzidine and 0.015% H_2O_2 in 0.05 mol/l Tris-HCl, pH 7.6.

Measurement of HHV-8 genome by real-time PCR

DNA was extracted from the lung, liver and spleen of CEP-treated and untreated mice. Copy number of KSHV ORF26 was measured with a Taqman real-time PCR[35] The real-time PCR assay used forward (5′-CTCGAATCCAACGGATTTGAC-3′) and reverse (5′-TGCTGCAGAATAGCGTGCC-3′) primers (Oligos Etc., Wilsonville, OR) and the fluorogenic Taqman probe (5′-CCATGGTCGTGCCGCAGCA-3′; PE Applied Biosystems, Foster City, CA) to amplify and detect a 74-base pair amplicon in the KSHV minor capsid protein gene (open reading frame 26, from nucleotides 47,311 to 47,384 of the KSHV genome).

Treatment of Balb/c mice with CEP

Eight-week-old female Balb/c mice were obtained from Clea Japan (Tokyo, Japan). Mice were treated with intraperitoneal injections of PBS or CEP (10 mg/kg per day) for 21 consecutive days. Splenocytes were harvested, counted the cell numbers and stained with anti-mouse CD3-FITC and anti-mouse CD19-PE (eBiosciences, San Diego, CA).The cells were analyzed on LSR II flow cytometer, and data were analyzed on FlowJo software.

Statistical analysis

All assays were performed in triplicates and expressed as mean values ± SE. The statistical significance of the differences observed between experimental groups was determined using the Student *t* test. *p* values less than 0.05 were considered significant.

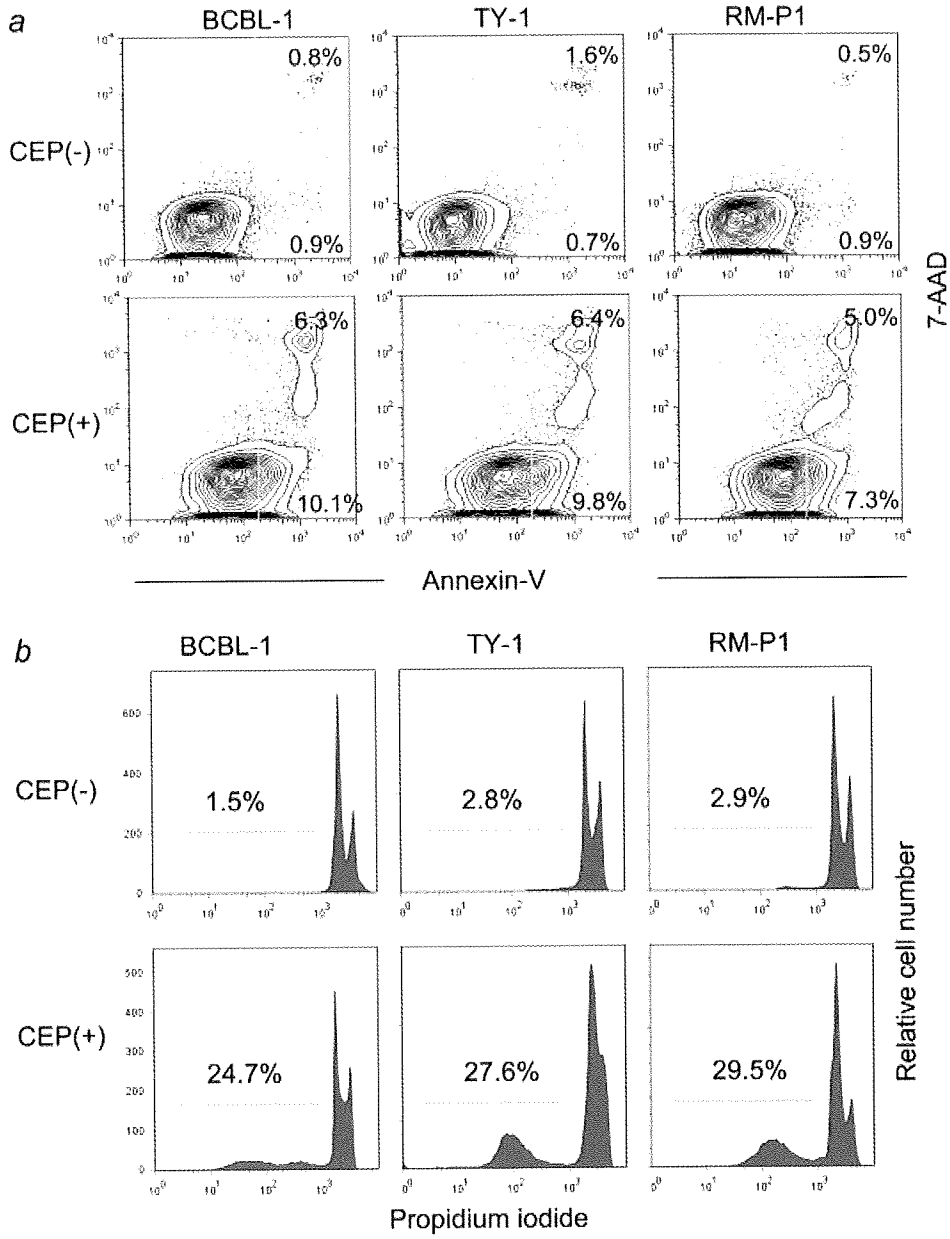

FIGURE 3 – CEP causes apoptosis of PEL cells. (*a*) CEP-induced apopotosis as detected by Annexin V and 7-AAD dual staining. The PEL cell lines BCBL-1, TY-1 and RM-P1 were treated with CEP (10 μg/ml) for 24 hr and were subsequently stained with Annexin-PE and 7-AAD before being analyzed by flow cytometry. (*b*) Apoptosis was determined by flow cytometric analysis of DNA fragmentation of PI stained nuclei. One representative result from 3 independent experiments is shown.

Results

CEP causes a dose-dependent inhibition of proliferation and apoptosis of PEL cell lines

We initially sought to determine whether CEP treatment leads to the inhibition of PEL cell proliferation. Three PEL cell lines (BCBL-1, TY-1 and RM-P1) and 3 non-PEL B cell lines (Ball-1, RAMOS and Raji) were cultured in the presence of 1, 3, 5 and 10 μg/ml CEP for 48 hr, and proliferation was analyzed by MTT assays. Figure 1 shows that as the dose of CEP increased from 1 to 10 μg/ml, cell growth inhibition increased in a dose-dependent fashion in all PEL cell lines and non-PEL B cell lines. PEL cell lines were more sensitive than non-PEL B cell lines against CEP treatment. In subsequent experiments, we determined whether the observed suppressive effects of CEP in MTT assay were due to induction of cell cycle arrest or apoptosis. As shown in Figure 2, CEP treatment for 18 hr induced cell cycle arrest with dose-dependent manner. We used Annexin V and 7-AAD dual staining to detect apoptosis. Annexin positive 7-AAD negative fraction represents the early phase of apoptosis whereas Annexin positive 7-AAD positive fraction represents the late phase of apoptosis and necrosis.[36] As shown in Figure 3*a*, 10 μg/ml CEP treatment for 24 hr caused apoptosis in all cell line tested. The sub-G1 population of cells (apoptotic cells)[28,37] increased with CEP treatment (Fig. 3*b*), indicating the PEL cells fell into apoptosis. Next, we measured the activation of caspase 3 to further confirm that CEP induced apoptosis in PEL cells. As shown in Figure 4, CEP treatment of PEL cells induced activation of caspase 3, a hallmark of cells undergoing apoptosis.[29]

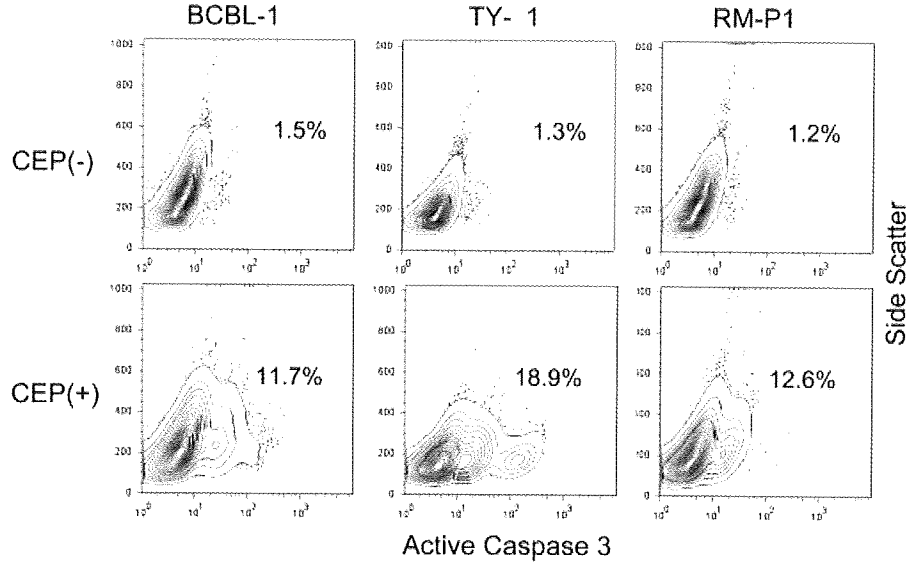

FIGURE 4 – CEP induces apoptosis of PEL cell *via* Caspase-3 dependent pathway. The PEL cells BCBL-1, TY-1 and RM-P1 were treated with CEP (10 μg/ml) for 24 hr and were subsequently stained with caspase-3 before being analyzed by flow cytometry. One representative result from 3 independent experiments is shown.

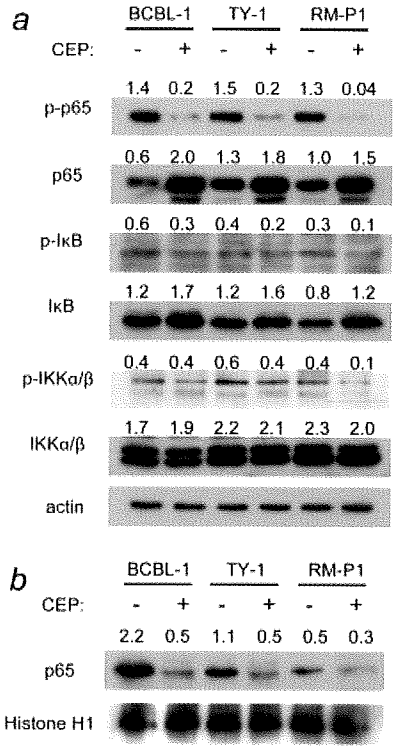

FIGURE 5 – Inhibitory effects of CEP on the expression of NF-κB pathways. (*a*) The PEL cell lines BCBL-1, TY-1 and RM-P1 were treated with CEP (10 μg/ml) for 24 hr and total proteins were extracted and Western blot was performed. The numbers indicate the relative expression of each protein level normalized with actin. (*b*) The PEL cell lines BCBL-1, TY-1 and RM-P1 were treated with CEP (10 μg/ml) for 24 hr and nuclear proteins were extracted and Western blot was performed to detect the NF-κB p65. The numbers indicate the relative expression of p65 normalized with Histone H1. One representative result from 3 independent experiments is shown.

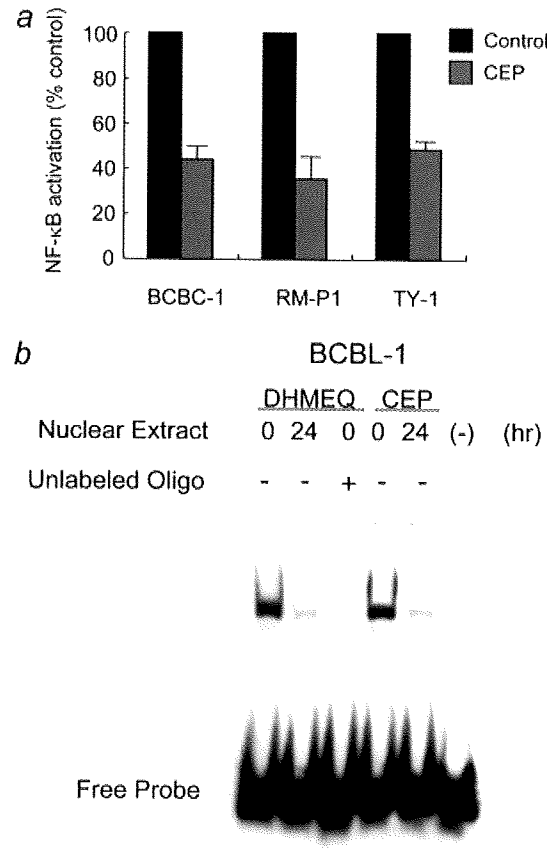

FIGURE 6 – Inhibition of NF-κB activation with CEP. (*a*) The PEL cell lines BCBL-1, TY-1 and RM-P1 were treated with CEP (10 μg/ml) for 24 hr and nuclear proteins were extracted and NF-kB activity was measured by ELISA. Data are expressed as a percentage of control. (*b*) BCBL-1 cells were treated with a specific NF-κB inhibitor, DHMEQ (10 μM) or CEP (10 μg/ml) for 24 hr and assessed for NF-κB DNA binding activity by EMSA using an NF-κB specific oligonucleotide probe. Shown as the mean ± S.D. from 3 independent experiments.

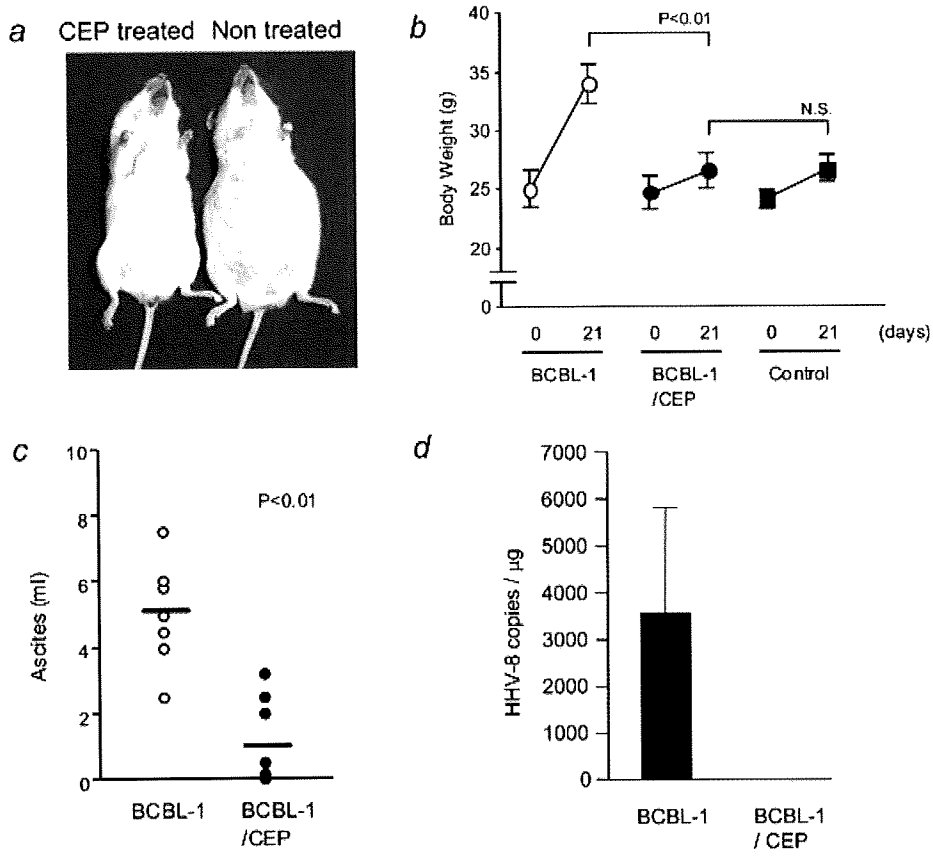

FIGURE 7 – Treatment of NOD/Scid/Jak3 deficient mice with CEP suppresses the development of KSHV-associated lymphoma *in vivo*. (*a*) A photograph of CEP-treated and nontreated ascites-bearing mice 3 weeks after being inoculated with BCBL-1 intraperitoneally. (*b*) The body weight of the mice inoculated with BCBL-1 cells and treated or untreated with CEP, shown as the mean ± S.D. from 7 mice. (*c*) The volume of ascites in mice inoculated with BCBL-1 cells and treated or untreated with CEP, shown as the mean ± S.D. from 7 mice. (*d*) Real-time PCR for KSHV genome. DNA was extracted from the lung, liver and spleen of CEP-treated and untreated mice. Copy number of KSHV ORF26 was measured with a Taqman real-time PCR. [Color figure can be viewed in the online issue, which is available at www.interscience.wiley.com.]

CEP efficiently blocks the constitutive NF-κB activity of PEL cell lines

Several reports have suggested that NF-κB can act as a survival factor and is required for the proliferation of PEL cells.[5,11,38] Because NF-κB is constitutively active in PEL cells,[9] we examined whether CEP inhibits NF-κB activation. When PEL cell lines were treated with 10 μg/ml CEP for 24 hr, the amount of phosphorylated p65 NF-κB protein was severely reduced; however, the amount of p65 NF-κB protein was rather increased, indicating that CEP suppresses NF-κB activity by suppressing the activation of p65 NF-κB (Fig. 5*a*). Suppression of p65 NF-κB activation blocks the nuclear translocation leads to the accumulation of p65 NF-κB protein. Untreated PEL cell lines constitutively expressed both total and phosphorylated IκB, the upstream of NF-κB. CEP treatment slightly reduced phosphorylated IκB and phosphorylated IKKα/β whereas total IκB was slightly increased, suggesting that inhibition of phosphorylation of IκB leads to stabilization of IκB by blocking degradation of IκB protein. Thus, CEP mainly inhibits the p65 NF-κB activation. Next, We fractioned nuclear protein and analyzed the expression of p65 by Western blotting (Fig. 5*b*) to confirm the p65 NF-κB suppression by CEP. When PEL cell lines were treated with 10 μg/ml CEP for 24 hr, the amount of nuclear p65 NF-κB protein was reduced as expected, indicating CEP suppresses NF-κB activity. To confirm that CEP could inhibit NF-κB activity in PEL cell lines, we measured the active NF-κB of nuclear extract by ELISA, and performed an EMSA with DIG labeled double-stranded NF-κB oligonucleotides (Fig. 6). Treatment with CEP suppressed the NF-κB activity in all cell lines tested (Fig. 6*a*). Treatment with DHMEQ, an NF-κB inhibitor, at a concentration of 10 μg/ml abrogated the constitutive NF-κB binding activity in BCBL-1 cells. CEP also abrogated the constitutive NF-κB binding activity (Fig. 6*b*). These results reveal that CEP blocks the constitutive NF-κB activity of PEL cells.

In vivo *effects of CEP on immunodeficient mice that had been inoculated with a PEL cell line*

As the above results suggested the efficacy of CEP for the treatment of PEL patients, we next examined the *in vivo* effects of CEP in an immunodeficient mice model. Severe immunodeficient, NOD/Scid/Jak3 deficient mice (NOJ mice)[33] were inoculated intraperitoneally with 7×10^6 BCBL-1 cells. BCBL-1 produced massive ascites within 3 weeks of inoculation (Fig. 7*a*), and body weight was significantly increased in all mice (Fig. 7*b*). As PEL is characterized by lymphomatous effusions of serous cavities and rarely presents with a definable tumor mass,[1,2] these mice are a clinically relevant PEL model. A dose of 10 mg/kg CEP in PBS or PBS alone was administrated *via* intraperitoneal injection on day 3 after cell inoculation and everyday thereafter for 21 days. CEP treated mice appeared to be healthy, with the same body weight as the nontumor inoculated mice and had a significantly lower volume of ascites (5.2 ± 1.5 ml *vs.* 1.1 ± 1.2 ml, $n = 7$ each, $p < 0.001$) (Fig. 7*b*).The body weight of the nontreated mice was significantly increased compared to that of the CEP treated mice (34.2 ± 1.7 g *vs.* 26.6 ± 1.4 g, $n = 7$, $p < 0.001$; Fig. 7*c*). DNA was extracted from the lung, liver and spleen of CEP-treated and